# Chapter 2
# Control Reconfiguration on Deadlocked Gimballed Thrust of Launch Vehicle

**Lei Liu and Yongji Wang**

**Abstract** An unprecedented challenge of the new generation launch vehicle control is its four parallel strap-on engines are oscillateable by the servomechanism. It increases the manoeuvrability of the vehicle and the control complexity simultaneously. The chapter investigates actuator failure compensation for new generation launch vehicle control. A control reconfiguration scheme of fault-tolerant control is developed to enhance the reliability of launch vehicle attitude control systems and prevent the control invalidation caused by the deadlock of the oscillating actuator, based on the congruity of the composite moment before and after the failure happens. This reconfiguration scheme is capable of utilizing the remaining control authority to achieve the desired performance in the presence of deadlock at certain detectable angle occurring in one or several actuators at unknown time instants.

**Keywords** Launch vehicle · Fault tolerance · Control reconfiguration · Attitude tracking

## 2.1 Introduction

Heavy lift launch vehicle (HLLV) is capable of lifting more than 14 tons into low earth orbit (LEO) and at least 5 tons to geostationary transfer orbit (GTO) than medium lift launch vehicles. The Chinese Government announced in its November 2000 white paper titled "China's Space Activities" that "the next generation of launch vehicles

L. Liu (✉) · Y. Wang
Key Laboratory of Ministry of Education for Image Processing and Intelligent Control,
School of Automation, Huazhong University of Science and Technology,
Wuhan, 430074, Hubei, People's Republic of China
e-mail: lei.liu.chn@gmail.com

Y. Wang
e-mail: wangyjch@hust.edu.cn

L. Liu et al. (eds.), *Applied Methods and Techniques for Mechatronic Systems*,
Lecture Notes in Control and Information Sciences 452,
DOI: 10.1007/978-3-642-36385-6_2, 

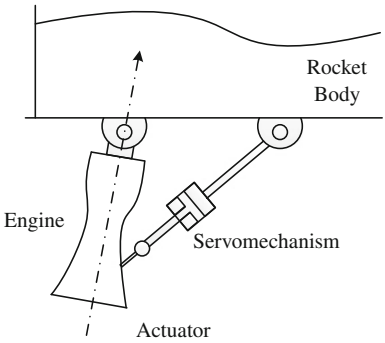


**Fig. 2.1** Gimballed thrust vector control system

with non-toxic, non-polluting, high-performance and low-cost qualities" [1] is able to deliver up to 25 tons payload into the LEO or 14 tons payload in the GTO. The new generation launch vehicle will be equipped with much powerful thrust to support heavier actual load to the target orbit.

The symbolical structure of the Gimballed Thrust Vector Control (GTVC) system in launch vehicle is shown in Fig. 2.1. The GTVC consists of power and servomechanism components, which manipulate the direction of the thrust to control the attitude and angular velocity of the vehicle. However, along with the additional gimballed thrust used on the new generation launch vehicle to increase the efficiency of the attitude control, the probability of engines failure is raised. Thus, to enhance the dependability of the launch vehicle, the fault-tolerance control method is a crucial part in vehicle attitude control.

The fault-tolerant control (FTC) of dynamic system is developed in accompany with the analytical redundancy-based fault diagnostics technology, and connects with the fault detection and diagnosis (FDD) module closely and ordinarily. The FTC is a certain kind of close-loop control system, which keeps the system stable with acceptable performance while the actuators or some parts of the system somehow fail [2].

There are two common manners for FTC, passive FTC and active FTC. Passive FTC is to design the proper controller with certain fixed structure and choose the parameters to satisfy both normal situation and failure conditions [3]. On the other hand, the controller should be adjusted after the failure occurred. Most of the active FTC requires FDD subsystem to provide the failure information of the system, to guarantee the priority of the failure. From the principle of the controller, we have following two kinds of the Active FTC ways. One is the Controller Gain Scheduling method, which designs the control law by choosing variant gain parameters based on the fault conditions. The other one is called Online Controller Design, which will make up a new controller structure with the proper parameters, which is called control reconfiguration method [4–6]. The common strategies for control reconfiguration method focusing on the controller parameters regulation are Pseudo-inverse method, Control mixer method, MIMO model self-adaptive method, and Quantitative feedback

theory (QFT), etc. [7–11]. Some other widely used control reconfiguration methods to regulate the structure of the controller while fault is occurred, are model-based control [12], model reference adaptive control [13], Conjugate Gradient Method [14], artificial neutral networks [15], T-S Fuzzy Models [16] etc. Comparing with the strategy proposed in this chapter, the above parameters based and structure-based fault tolerant control methods are based on model of failure launch vehicle. And the controller is designed both for the normal flight conditions and fault occurred conditions [17, 18]. However, the model of the failure vehicle is often hard to be obtained, because of the randomness of the occurrence. Moreover, the model-based control method needs huge precomputation to determine the structure and parameters of the controller, and then load them to the vehicle computer. The regulation will be always hysteretic and stiff. Therefore, in this chapter, we tend to provide a different FTC strategy to reconfigure the control action immediately when the fault is occurred.

The Passive FTC method is essential to design a robust close-loop controller to guarantee the stability of the failure system, but it sacrifices the performance of the system. However, the Active FTC needs to deal with the FDD and FTC problem at the same time. Therefore, in our chapter, the FDD module and fault information is assumed available from the servomechanism directly before the control reconfiguration FTC design.

The structure of the chapter is organized as follows: First, a nonlinear launch vehicle model that incorporates independently adjustable oscillating angles of both core engines and strap-on engines is presented and linearized to describe the vehicle's pitching, yawing, and rolling motion. The dynamic analysis and linearizing process are discussed in detail in Appendix. Then, the proposed reconfiguration scheme is provided to the linear vehicle model in the presence of servomechanism malfunction during operation. Furthermore, the inherent stability of the system is analyzed based on the distribution of the roots of its eigen-equation. The Nyquist curves and Bode diagrams are used to study the system's stability after the proper frequency correction. Based on the proper attitude controller, the reconfigurability analysis is derived. The ability of the control reconfiguration is analyzed under some practical assumptions, to study the tolerable range of the servomechanism to be deadlocked. At last, simulation results are presented to assess the effectiveness of this reconfiguration failure compensation design.

## 2.2 Problem Statement and Preliminaries

As described in Fig. 2.2, the attitude of the strap-on boosted Launch Vehicle has three basic orientations in the rocket coordinate system, which are called pitching, yawing, and rolling channels in the attitude control principles, separately.

For the strap-on boosted Launch Vehicle, the first stage composes with the strap-on thrusts around the body and the core thrusts in the center, of which the gimballed thrusts are the essential actuators of each channel and they affect the attitude of the launch vehicle. Therefore, any malfunction on actuators will cause serious disasters.

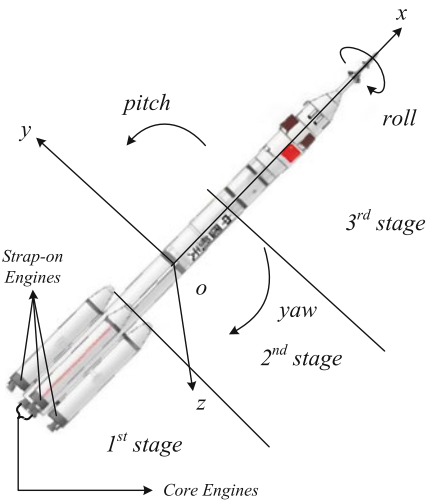


**Fig. 2.2** Basic attitude angle and stages of launch vehicle

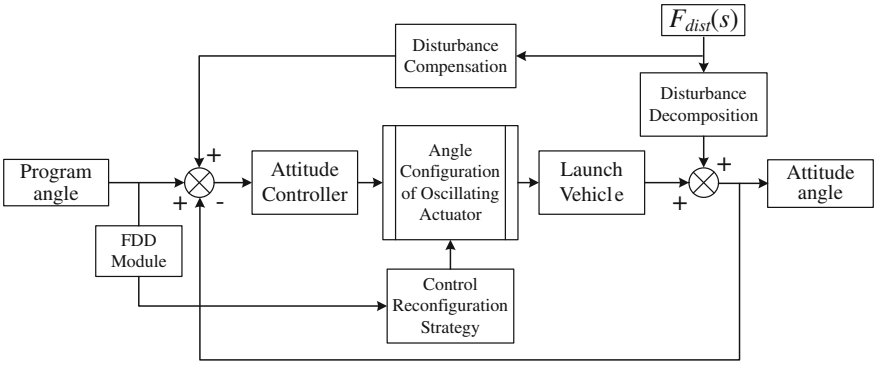


**Fig. 2.3** Brief control and reconfiguration structure diagram

Generally, the common actuator failures happen on the servomechanism and the thrust engines. However, the thrust failure would be fatal and irreversible, because the loss of thrust force will affect the initial track by the guidance process. Thus, in this chapter, the servomechanism failure problem is concerned, particularly the gimballed mechanism is deadlocked [19]. In this situation, the vehicle will lose its control stability immediately. However, the propulsion of the vehicle is still maintained. The presented control reconfiguration method is provided to maintain the control action by the remaining control authority to achieve the desired performance.

The brief control and reconfiguration structure is designed to achieve the attitude tracking control and fault-tolerance functions at the same time (see Fig. 2.3). In this structure, the system input is the program angles of the attitude, which is generated from the guiding system. After that is the attitude controller module. The

frequency-domain method is widely used in the stable attitude controller design, specially for the inherent instable launch vehicle model, because of its proven reliability. Practically, the disturbance always existed because of the wind and air, and assumed detectable or observable. The direct compensation method will be convenient and effective, which is not the essential problem of this chapter.

On the other hand, the fault-tolerant system is designed to provide service in the presence of faults. Providing redundant manipulation is a common method of recovering from faults, but it is not feasible in cases where space or weight restrictions limit the amount of room available for spares, for instance, the deep-space probe and the launch vehicle. A possible fault recovery method under these circumstances is to reconfigure the control actions by the existing equipments [20, 21].

At first, the failed actuator and its state will be detected by the servo feedback module to provide the prior information for control reconfiguration of the gimballed actuators. Furthermore, the system dynamics and the architectural feature of the actuators are the essential factors as well. Therefore, the further study is constructed by the upper problems.

## 2.3 Dynamic Model

The dynamic model of the launch vehicle is considered as a variable mass rigid body. Its dynamic motion can be obtained from Newton's second law which states that the summation of all external forces acting on a body is equal to the time rate of change of the momentum of the body, and the summation of the external moments acting on the body is equal to the time rate of change of the moment of angular momentum. For the flight dynamics, normally, an axis system fixed to the Earth can be used as an inertial reference frame. Newton's second law can be expressed in the following equations [22]:

$$\begin{cases} \sum \mathbf{F} = \frac{\mathrm{d}}{\mathrm{d}t}(m\mathbf{V}) = \mathbf{G} + \mathbf{P} + \mathbf{A} + \mathbf{C} + \mathbf{S} + \mathbf{E} + \mathbf{R} \\ \sum \mathbf{M} = \frac{\mathrm{d}}{\mathrm{d}t}\mathbf{H} = \frac{\mathrm{d}}{\mathrm{d}t}(J\omega) + \omega \times (J\omega) \end{cases} \tag{2.1}$$

If we let $\delta m$ be an element of mass of the vehicle, $\mathbf{V}$ be the velocity of the elemental mass relative to an inertial frame, and $\delta\mathbf{F}$ be the composite force acting on the elemental mass; then Newton's second law yields:

$$\delta\mathbf{F} = \delta m \frac{\mathrm{d}\mathbf{V}}{\mathrm{d}t} \tag{2.2}$$

Similarly, we consider about the composite moment on the elemental mass of the vehicle $\delta\mathbf{M}$ and the moment of inertia $\delta J$.

$$\frac{\mathrm{d}}{\mathrm{d}t}(J\omega) = \delta J \frac{\mathrm{d}\omega}{\mathrm{d}t} \tag{2.3}$$

Therefore, the dynamics including the motion of the mass center and the rotation around the mass center in the three axis directions (see Fig. 2.2) can be presented as:

$$\begin{cases} \delta m \frac{\mathrm{d}\mathbf{V}}{\mathrm{d}t} = \sum \mathbf{F}_x = \mathbf{F}_{Gx} + \mathbf{F}_{Px} + \mathbf{F}_{Ax} + \mathbf{F}_{Cx} + \mathbf{F}_{Ex} + \mathbf{F}_x \\ \delta m \mathbf{V} \frac{\mathrm{d}\theta}{\mathrm{d}t} = \sum \mathbf{F}_y = \mathbf{F}_{Gy} + \mathbf{F}_{Py} + \mathbf{F}_{Ay} + \mathbf{F}_{Cy} + \mathbf{F}_{Ey} + \mathbf{F}_y \\ -\delta m \mathbf{V} \frac{\mathrm{d}\sigma}{\mathrm{d}t} = \sum \mathbf{F}_z = \mathbf{F}_{Gz} + \mathbf{F}_{Pz} + \mathbf{F}_{Az} + \mathbf{F}_{Cz} + \mathbf{F}_{Ez} + \mathbf{F}_z \\ \delta J_x \frac{\mathrm{d}\omega_x}{\mathrm{d}t} + (\delta J_z - \delta J_y)\omega_z\omega_y = \sum \mathbf{M}_x = \mathbf{M}_{Ax} + \mathbf{M}_{Cx} + \mathbf{M}_{Ex} + \mathbf{M}_x \\ \delta J_y \frac{\mathrm{d}\omega_y}{\mathrm{d}t} + (\delta J_x - \delta J_z)\omega_x\omega_z = \sum \mathbf{M}_y = \mathbf{M}_{Ay} + \mathbf{M}_{Cy} + \mathbf{M}_{Ey} + \mathbf{M}_y \\ \delta J_z \frac{\mathrm{d}\omega_z}{\mathrm{d}t} + (\delta J_y - \delta J_x)\omega_y\omega_x = \sum \mathbf{M}_z = \mathbf{M}_{Az} + \mathbf{M}_{Cz} + \mathbf{M}_{Ez} + \mathbf{M}_z \end{cases} \tag{2.4}$$

Based on the equations above, the derivation of the formula for nonlinear modeling of the vehicle and its linearizing process is studied in the Appendix. Then, the linear dynamic model of the vehicle can be formulated in the following three channels, corresponding to the three axis directions before.
In pitching channel:

$$\begin{cases} \Delta\dot{\theta} = c_1^{\varphi}\Delta\alpha + c_2^{\varphi}\Delta\theta + c_{3\text{core}}^{\varphi}\delta_{\varphi}^{\text{core}} + c_{3\text{core}}^{\prime\varphi}\ddot{\delta}_{\varphi}^{\text{core}} + c_{3\text{strap-on}}^{\varphi}\delta_{\varphi}^{\text{strap-on}} \\ + c_{3\text{strap-on}}^{\prime\varphi}\ddot{\delta}_{\varphi}^{\text{strap-on}} + c_1^{\prime\varphi}\alpha_w + \overline{F}_{yc} \\ \Delta\ddot{\varphi} + b_1^{\varphi}\Delta\dot{\varphi} + b_2^{\varphi}\Delta\alpha + b_{3\text{core}}^{\varphi}\delta_{\varphi}^{\text{core}} + b_{3\text{core}}^{\prime\varphi}\ddot{\delta}_{\varphi}^{\text{core}} + b_{3\text{strap-on}}^{\varphi}\delta_{\varphi}^{\text{strap-on}} \\ + b_{3\text{strap-on}}^{\prime\varphi}\ddot{\delta}_{\varphi}^{\text{strap-on}} + b_2^{\varphi}\alpha_w = \overline{M}_z \\ \Delta\varphi = \Delta\alpha + \Delta\theta \end{cases} \tag{2.5}$$

in yawing channel:

$$\begin{cases} \dot{\sigma} = c_1^{\psi}\beta + c_2^{\psi}\sigma + c_{3\text{core}}^{\psi}\delta_{\psi}^{\text{core}} + c_{3\text{core}}^{\prime\psi}\ddot{\delta}_{\psi}^{\text{core}} + c_{3\text{strap-on}}^{\psi}\delta_{\psi}^{\text{strap-on}} + c_{3\text{strap-on}}^{\prime\psi}\ddot{\delta}_{\psi}^{\text{strap-on}} \\ + c_1^{\prime\psi}\beta_w - \overline{F}_{zc} \\ \ddot{\psi} + b_1^{\psi}\dot{\psi} + b_2^{\psi}\beta + b_{3\text{core}}^{\psi}\delta_{\psi}^{\text{core}} + b_{3\text{core}}^{\prime\psi}\ddot{\delta}_{\psi}^{\text{core}} + b_{3\text{strap-on}}^{\psi}\delta_{\psi}^{\text{strap-on}} + b_{3\text{strap-on}}^{\prime\psi}\ddot{\delta}_{\psi}^{\text{strap-on}} \\ + b_2^{\psi}\beta_w = \overline{M}_y \\ \psi = \beta + \sigma \end{cases} \tag{2.6}$$

and in rolling channel:

$$\ddot{\gamma} + d_1\dot{\gamma} + d_{3\text{core}}\delta_{\gamma}^{\text{core}} + d'_{3\text{core}}\ddot{\delta}_{\gamma}^{\text{core}} + d_{3\text{strap-on}}\delta_{\gamma}^{\text{strap-on}} + d'_{3\text{strap-on}}\ddot{\delta}_{\gamma}^{\text{strap-on}} = \overline{M}_x \tag{2.7}$$

In the equations above, the coefficients of the linear system is decided by the certain physics parameters as in the Appendix. Here, we assume that the variation of the vehicle motion is small in a short-time period. Therefore, by the small disturbances linearizing method, the complicated nonlinear system can be indicated by the variate coefficients linear system approximately.

Notice that, the oscillation angles in the system differential equations, such as $\delta_{\varphi}^{\text{strap-on}}$, $\delta_{\varphi}^{\text{core}}$, $\delta_{\psi}^{\text{strap-on}}$, $\delta_{\psi}^{\text{core}}$, etc., are the equivalent angles of the vehicle and cannot

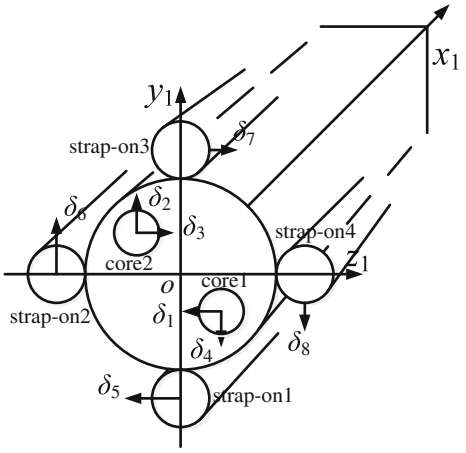


**Fig. 2.4** Schematic diagram of propellant rocket engines

reflect the physics property or internal relationship between the oscillation angles of the actuators. Dr. Wu, who was the President of China Academy of Launch Vehicle Technology (CALT), has revealed the outline of Chinese new generation launch vehicle in [23] and discussed the structure of the first stage with four strap-on engines and two moveable core engines, which is different from the previous design of the "Long March" launch vehicles.

As shown in Fig. 2.4, $ox_1y_1z_1$ is the rocket coordinate system from the bottom of the launch vehicle. The "core1" and "core2" stand for two core thrusts, and "strap-on1" to "strap-on4" are symbols of four strap-on thrusts. The "strap-on" thrusts are also called booster engines in some literatures. The core engines are in the first and third quartiles in $oy_1z_1$ plane, while four strap-on engines are on $y$, $z$ axis of the plane. The movements of the gimballed thrusts in different directions are labeled by $\delta_i$ with the arrows denoting their positive orientations.

Generally, to simplify the kinematic and dynamic models of the vehicle, we use the equivalent oscillating angle $\delta_\varphi^{\text{core}}$ and $\delta_\varphi^{\text{strap-on}}$ as the equivalent angles to rewrite the dynamic model of the launch vehicle with core stages and the strap-on stages, which denote the combined oscillating angle of the physical helms of the engines. Obviously, the corresponding relationship between the equivalent angles: $\delta_\varphi^{\text{core}}$, $\delta_\varphi^{\text{strap-on}}$ and the oscillating angles of the engines: $\delta_i, i = 1, 2, \ldots, 8$ will satisfy the following relationships:

For core stages:

$$\begin{cases} \delta_\varphi^{\text{core}} = \delta_4 - \delta_2 \\ \delta_\psi^{\text{core}} = \delta_3 - \delta_1 \\ \delta_\gamma^{\text{core}} = (\delta_1 + \delta_2 + \delta_3 + \delta_4)/2 \end{cases} \tag{2.8}$$

For strap-on stages:

$$\begin{cases} \delta_{\varphi}^{\text{strap-on}} = (\delta_8 - \delta_6)/2 \\ \delta_{\psi}^{\text{strap-on}} = (\delta_7 - \delta_5)/2 \\ \delta_{\gamma}^{\text{strap-on}} = (\delta_5 + \delta_6 + \delta_7 + \delta_8)/4 \end{cases} \tag{2.9}$$

## 2.4 Control Reconfiguration Strategies

In this section, the actuator deadlock compensation strategies based on the linearized dynamic model are researched. First, we study the correlation of the actuators to look for the necessary redundancy for the failure actuator compensation. Then, the control reconfiguration strategies of different faulty conditions are derived and formulated, which are the essential results of the chapter.

### *2.4.1 Association Analysis*

To study the association of the actuators of the strap-on and core thrusts, the state space representation of the system can be established as follows, from the linearized dynamic model is:
The state equation in the pitching channel is:

$$\begin{bmatrix} \dot{\theta} \\ \dot{\varphi} \\ \ddot{\varphi} \end{bmatrix} = \begin{bmatrix} c_2^{\varphi} - c_1^{\varphi} & c_1^{\varphi} & 0 \\ 0 & 0 & 1 \\ b_2^{\varphi} & -b_2^{\varphi} & -b_1^{\varphi} \end{bmatrix} \begin{bmatrix} \theta \\ \varphi \\ \dot{\varphi} \end{bmatrix} + \begin{bmatrix} \frac{c_{3\text{strap-on}}^{\varphi}}{2} & -\frac{c_{3\text{strap-on}}^{\varphi}}{2} & c_{3\text{core}}^{\varphi} & -c_{3\text{core}}^{\varphi} \\ 0 & 0 & 0 & 0 \\ -\frac{b_{3\text{strap-on}}^{\varphi}}{2} & \frac{b_{3\text{strap-on}}^{\varphi}}{2} & -b_{3\text{core}}^{\varphi} & b_{3\text{core}}^{\varphi} \end{bmatrix} \cdot \begin{bmatrix} \delta_8 \\ \delta_6 \\ \delta_4 \\ \delta_2 \end{bmatrix} + \begin{bmatrix} c_1'^{\varphi} \\ 0 \\ -b_2^{\varphi} \end{bmatrix} \alpha_w + \begin{bmatrix} \bar{F}_{yc} \\ 0 \\ \bar{M}_z \end{bmatrix} \tag{2.10}$$

The one in the yawing channel is:

$$\begin{bmatrix} \dot{\sigma} \\ \dot{\psi} \\ \ddot{\psi} \end{bmatrix} = \begin{bmatrix} c_2^{\psi} - c_1^{\psi} & c_1^{\psi} & 0 \\ 0 & 0 & 1 \\ b_2^{\psi} & -b_2^{\psi} & -b_1^{\psi} \end{bmatrix} \begin{bmatrix} \sigma \\ \psi \\ \dot{\psi} \end{bmatrix} + \begin{bmatrix} \frac{c_{3\text{strap-on}}^{\psi}}{2} & -\frac{c_{3\text{strap-on}}^{\psi}}{2} & c_{3\text{core}}^{\psi} & -c_{3\text{core}}^{\psi} \\ 0 & 0 & 0 & 0 \\ -\frac{b_{3\text{strap-on}}^{\psi}}{2} & \frac{b_{3\text{strap-on}}^{\psi}}{2} & -b_{3\text{core}}^{\psi} & b_{3\text{core}}^{\psi} \end{bmatrix} \cdot \begin{bmatrix} \delta_7 \\ \delta_5 \\ \delta_3 \\ \delta_1 \end{bmatrix} + \begin{bmatrix} c_1'^{\psi} \\ 0 \\ -b_2^{\psi} \end{bmatrix} \beta_w + \begin{bmatrix} -\overline{F}_{zc} \\ 0 \\ \overline{M}_y \end{bmatrix} \tag{2.11}$$

And in the rolling channel is:

$$\begin{bmatrix} \dot{\gamma} \\ \ddot{\gamma} \end{bmatrix} = \begin{bmatrix} 0 & 1 \\ 0 & -d_1 \end{bmatrix} \begin{bmatrix} \gamma \\ \dot{\gamma} \end{bmatrix} + \begin{bmatrix} 0 & 0 \\ -d_{3\text{strap-on}} & -d_{3\text{core}} \end{bmatrix} \cdot \begin{bmatrix} \frac{\mathbf{1}}{\mathbf{4}}_{1\times 4} & 0 \\ 0 & \frac{\mathbf{1}}{\mathbf{2}}_{1\times 4} \end{bmatrix} \begin{bmatrix} \delta_5 \\ \vdots \\ \delta_8 \\ \delta_1 \\ \vdots \\ \delta_4 \end{bmatrix} + \begin{bmatrix} 0 \\ \bar{M}_x \end{bmatrix} \tag{2.12}$$

From the state equation representation of the launch vehicle, the oscillating angles of the core thrusts are $\delta_2$ and $\delta_4$, and the ones of strap-on thrusts are $\delta_6$ and $\delta_8$, which will give the thrust in pitching and rolling channels. On the other hand, the oscillating angles $\delta_1$, $\delta_3$, $\delta_5$, and $\delta_7$ of the core and strap-on thrusts support for the motion in yawing and rolling channels simultaneously.

Usually, the rolling motion is always very little and control ignored. Considering the situation that there exists the rolling motion of the launch vehicle, the motion related actuators will be interchanged during the flight process. The system will become coupled and complicated. Therefore, the condition of the following results of control reconfiguration strategies is to eliminate the rolling motion of the launch vehicle by the attitude controller. Then the states coupling barely existed between the rolling channel and other two channels.

### *2.4.2 Control Reconfiguration of One Engine Deadlock*

As we discussed before, the gimballed thrusts consist of the power and actuation components that control the main engine's direction to steer the vehicle in the right direction.

Without loss of generality, we choose the pitching channel as an example for our analysis. Considering a fault scenario that the oscillating angle of the strap-on thrust No.2 (strap-on2 in Fig. 2.4) $\delta_6$ is deadlocked in a constant value $\delta_6' = \tilde{\delta}_6$, the distinction between the deadlocked angle and normal angle is: $\Delta\delta_6 = \delta_6' - \delta_6 = \tilde{\delta}_6 - \delta_6$. From the state space representation of the dynamic model in Eqs. (2.10), (2.11), and (2.12), the oscillation angle $\delta_6$ of the failed strap-on engine No. 2 will affect the motion in pitching and rolling channels simultaneously, except the yawing channel. To guarantee the vehicle's trajectory tracking precision, the adequate manipulation for ce and moment from the normal operated thrust is required to maintain the control authority and compensate the appended moments from the deadlocked engine, and the composite control moment remaining on the vehicle.

First of all, we propose the following parameters: the thrust of each core engine is $N_c$, with the relative oscillation angles: $\delta_1$, $\delta_2$, $\delta_3$, and $\delta_4$, and the thrust of each strap-on engine is $N_s$ with the relative oscillation angles: $\delta_5$, $\delta_6$, $\delta_7$, and $\delta_8$. The

distance from the oscillating axis of the engine to the center of mass is L, and the vertical distances from direct-axis to the strap-on and core thrusts are $R$ and $r$, correspondingly. Since the oscillating angle is always less than eight degrees, the following equations can be obtained approximately:

$$\sin\delta \approx \delta \tag{2.13}$$

Then, the approximate control moments of gimballed thrusts to each axis in space are:

$$\begin{cases} M_{xc} = N_s(\delta_5 + \delta_6 + \delta_7 + \delta_8)R + N_c(\delta_1 + \delta_2 + \delta_3 + \delta_4)r \\ M_{yc} = [N_s(\delta_5 - \delta_7) + N_c(\delta_1 - \delta_3)]L \\ M_{zc} = [N_s(\delta_8 - \delta_6) + N_c(\delta_4 - \delta_2)]L \end{cases} \tag{2.14}$$

After that, assuming the reconfigured angles of the gimballed thrusts except failed strap-on2 are $\delta'_1$ to $\delta'_8$, which are the expected angles to keep the control moment. Then, balance equations of the control moment are:

$$\begin{cases} N_s(\delta_5 + \delta_6 + \delta_7 + \delta_8)R + N_c(\delta_1 + \delta_2 + \delta_3 + \delta_4)r = N_s(\delta'_5 + \tilde{\delta}_6 + \delta'_7 + \tilde{\delta}_8)R \\ +N_c(\delta'_1 + \delta'_2 + \delta'_3 + \delta'_4)r \\ [N_s(\delta_5 - \delta_7) + N_c(\delta_1 - \delta_3)]\,L = [N_s(\delta'_5 - \delta'_7) + N_c(\delta'_1 - \delta'_3)]L \\ [N_s(\delta_8 - \delta_6) + N_c(\delta_4 - \delta_2)]\,L = [N_s(\tilde{\delta}_8 - \tilde{\delta}_6) + N_c(\delta'_4 - \delta'_2)]L \end{cases} \tag{2.15}$$

Since the oscillating angle $\delta_6$ would not influence the state of the yawing channel, the oscillating angles in the yawing channel satisfy: $\delta'_1 = \delta_1$, $\delta'_3 = \delta_3$, $\delta'_5 = \delta_5$, and $\delta'_7 = \delta_7$.

Thus, the Eq. (2.15) can be reduced as follows:

$$\begin{cases} N_s(\delta_8 + \delta_6 - \delta'_8 - \tilde{\delta}_6)R = N_c(\delta'_4 + \delta'_2 - \delta_4 - \delta_2)r \\ N_s(\delta_8 - \delta_6 - \delta'_8 + \tilde{\delta}_6) = N_c(\delta'_4 - \delta'_2 - \delta_4 + \delta_2) \end{cases} \tag{2.16}$$

Moreover, there is a proportional relation between the corresponded core thrusts and strap-on thrusts, which is denoted by a parameter $k$: $\delta_8 = k \cdot \delta_4$ and $\delta'_8 = k \cdot \delta'_4$.

$$\begin{cases} \dfrac{N_s}{N_c}\dfrac{R}{r}(\delta_8 + \delta_6 - \tilde{\delta}_6) + \delta_4 + \delta_2 = (1 + \dfrac{N_s}{N_c}\dfrac{R}{r}k)\delta'_4 + \delta'_2 \\ \dfrac{N_s}{N_c}(\delta_8 - \delta_6 + \tilde{\delta}_6) + \delta_4 - \delta_2 = (1 + \dfrac{N_s}{N_c}k)\delta'_4 - \delta'_2 \end{cases} \tag{2.17}$$

From the simultaneous equations above, the reconfigured oscillating angles should be regulated as follow, with the failed strap-on thrust No.2 deadlocked at $\tilde{\delta}_6$.

$$\begin{cases} \delta'_6 = \tilde{\delta}_6 = \delta_6 + \Delta\delta_6 \\ \delta'_8 = \delta_8 - \dfrac{N_s(R-r)k}{[2N_c r + N_s(R+r)k]}\Delta\delta_6 \\ \delta'_2 = \delta_2 - \dfrac{N_s}{N_c}\dfrac{N_c(R+r)+2N_s kR}{[2N_c r + N_s(R+r)k]}\Delta\delta_6 \\ \delta'_4 = \delta_4 - \dfrac{N_s(R-r)}{[2N_c r + N_s(R+r)k]}\Delta\delta_6 \end{cases} \tag{2.18}$$

In which, $N_s$, $N_c$, $R$, $r$, and $k$ are the fundamental parameters and the constants given before. $\Delta\delta_6$ is a determined quantity to describe the deviation of the deadlocked engine.

The Eq. (2.18) denotes that when the strap-on thrust No. 2 is deadlocked at a certain angle, other normal working engines, such us the strap-on thrust No.4, core thrust No.2, and core thrust No.4 should regulate to a relative angles to maintain the control moment of the pitching and rolling channels. The regulative angles are relative to the scale of the launch vehicle $R$ and $r$, the thrust power of strap-on thrusts $N_s$, and core thrusts $N_c$ and the proportional relationship between the oscillating angles $k$. On the other hand, the oscillating angles of other four engines: strap-on1 and strap-on3, core1 and core3, should retain their state before.

The similar results of other engines will be achieved in yawing and rolling channels because of the symmetry of the vehicle.

### *2.4.3 Control Reconfiguration of Two Engines Deadlocked*

From analysis of one thrust deadlocked situation, we find that the control reconfiguration is the independent and symmetric process between the pitching and yawing channels based on the no-rolling assumption. The symmetry of the launch vehicle makes the yawing channel identical to the pitching channel. Thus, we can separate the two thrusts deadlocked analysis into two situations:

(I) Two failed thrusts are in different channels
(II) Two failed thrusts are in the same channel.

In situation (I), it is obviously to obtain the result that we can establish two groups of simultaneous equations in pitching and yawing channels relatively to guarantee that the control moment of the launch vehicle is kept invariable. Then the solutions of the equations are the reconfigured oscillating angles we need. So, we emphasize on the second situation that two deadlocked thrusts are in the same channel.

Considering the pitching channel without loss of generality, we choose strap-on2 and strap-on4 corresponding to the oscillating angles $\delta_6$ and $\delta_8$ for example. They are assumed to be deadlocked at the certain angle $\tilde{\delta}_6$ and $\tilde{\delta}_8$. Thus,

$$\begin{aligned} \delta'_6 &= \tilde{\delta}_6 = \delta_6 + \Delta\delta_6 \\ \delta'_8 &= \tilde{\delta}_8 = \delta_8 + \Delta\delta_8 \end{aligned} \tag{2.19}$$

Similarly, based on the assumption of Eq. (2.13), the corresponding balance relation of the control moments satisfy the Eq. (2.14) as well. Then, substitute the failure occurred angle $\tilde{\delta}_6$ and $\tilde{\delta}_8$ in Eq. (2.14) by Eq. (2.19).

$$\begin{cases} N_s(\delta_5 + \delta_6 + \delta_7 + \delta_8)R + N_c(\delta_1 + \delta_2 + \delta_3 + \delta_4)r = N_s(\delta'_5 + \tilde{\delta}_6 + \delta'_7 + \tilde{\delta}_8)R \\ +N_c(\delta'_1 + \delta'_2 + \delta'_3 + \delta'_4)r \\ \left[N_s(\delta_5 - \delta_7) + N_c(\delta_1 - \delta_3)\right]L = [N_s(\delta'_5 - \delta'_7) + N_c(\delta'_1 - \delta'_3)]L \\ [N_s(\delta_8 - \delta_6)L + N_c(\delta_4 - \delta_2)]\,L = [N_s(\tilde{\delta}_8 - \tilde{\delta}_6) + N_c(\delta'_4 - \delta'_2)]L \end{cases} \tag{2.20}$$

The oscillating angles performing in the yawing channel: $\delta_1$, $\delta_3$, $\delta_5$, and $\delta_7$ can be removed.

$$\begin{cases} N_s(\delta_8 + \delta_6 - \tilde{\delta}_8 - \tilde{\delta}_6)R = N_c(\delta'_4 + \delta'_2 - \delta_4 - \delta_2)r \\ N_s(\delta_8 - \delta_6 - \tilde{\delta}_8 + \tilde{\delta}_6) = N_c(\delta'_4 - \delta'_2 - \delta_4 + \delta_2) \end{cases} \tag{2.21}$$

However, because the strap-on thrusts are both deadlocked, the proportion relation $k$ between strap-on and core thrust is noneffective.

Solving the Eq. (2.21), we can obtain the reconfigured oscillating angles of the core engines in pitching channel:

$$\begin{cases} \delta'_2 = \delta_2 - \frac{N_s}{2N_c}\left(\frac{R}{r} + 1\right)\Delta\delta_6 - \frac{N_s}{2N_c}\left(\frac{R}{r} - 1\right)\Delta\delta_8 \\ \delta'_4 = \delta_4 - \frac{N_s}{2N_c}\left(\frac{R}{r} - 1\right)\Delta\delta_6 - \frac{N_s}{2N_c}\left(\frac{R}{r} + 1\right)\Delta\delta_8 \end{cases} \tag{2.22}$$

Therefore, the normal operative thrusts need to be regulated according to Eq. (2.22) to compensate the control force by the failed thrusts to maintain the competent operation for attitude manipulation.

Moreover, consider another situation that the deadlocked thrusts belongs to strap-on booster and core booster, separately. Assume they are strap-on2 and core2, for instance. So, we have the fault condition description in Eq. (2.23)

$$\begin{cases} \delta'_2 = \tilde{\delta}_2 = \delta_2 + \Delta\delta_2 \\ \delta'_6 = \tilde{\delta}_6 = \delta_6 + \Delta\delta_6 \end{cases} \tag{2.23}$$

And the regulated equations are:

$$\begin{cases} N_s(\delta_8 + \delta_6 - \delta'_8 - \tilde{\delta}_6)R = N_c(\delta'_4 + \tilde{\delta}_2 - \delta_4 - \delta_2)r \\ N_s(\delta_8 - \delta_6 - \delta'_8 + \tilde{\delta}_6) = N_c(\delta'_4 - \tilde{\delta}_2 - \delta_4 + \delta_2) \end{cases} \tag{2.24}$$

Then solving the equations above, we have:

$$\begin{cases} \delta'_4 = \delta_4 + \frac{2N_s R}{N_c(R-r)}\Delta\delta_6 + \frac{R+r}{R-r}\Delta\delta_2 \\ \delta'_8 = \delta_8 - \frac{R+r}{R-r}\Delta\delta_6 - \frac{2N_c r}{N_s(R-r)}\Delta\delta_2 \end{cases} \tag{2.25}$$

The control reconfiguration strategy is obtained.

Finally, consider about the situation that the deadlocked thrusts are strap-on2 and core4.

$$\begin{cases} \delta'_4 = \tilde{\delta}_4 = \delta_4 + \Delta\delta_4 \\ \delta'_6 = \tilde{\delta}_6 = \delta_6 + \Delta\delta_6 \end{cases} \tag{2.26}$$

The regulated equations are:

$$\begin{cases} N_s(\delta_8 + \delta_6 - \delta'_8 - \tilde{\delta}_6)R = N_c(\tilde{\delta}_4 + \delta'_2 - \delta_4 - \delta_2)r \\ N_s(\delta_8 - \delta_6 - \delta'_8 + \tilde{\delta}_6) = N_c(\tilde{\delta}_4 - \delta'_2 - \delta_4 + \delta_2) \end{cases} \tag{2.27}$$

The solution of the equations is:

$$\begin{cases} \delta'_2 = \delta_2 + \frac{R-r}{R+r}\Delta\delta_4 - \frac{2N_s R}{N_c(R+r)}\Delta\delta_6 \\ \delta'_8 = \delta_8 - \frac{2N_c r}{N_s(R+r)}\Delta\delta_4 - \frac{R-r}{R+r}\Delta\delta_6 \end{cases} \tag{2.28}$$

### *2.4.4 Control Reconfiguration of More Than Two Engines Deadlocked*

From the state space equations of the launch vehicle in Eqs. (2.10) and (2.11), four engines are implemented to provide the thrust power and control its attitude for the pitching and yawing channel, respectively. First, if there are three thrusts failed in the same channel, the vehicle will be a single-input but multi-output system. In this situation, the lack of control process will break the equilibrium of the moment in the corresponding channel and produce the trend of rotational motion. Then, the attitude of the vehicle will be unable to regulate. Therefore, it is forbidden that there are three engines deadlocked at the same time in the same channel. Obviously, it is meaningless if more than three thrusts are failed in the six engines driving the launch vehicle. The critical situation that the vehicle is recoverable is two thrusts failed in the same channel.

After that, considering the situation that more than two thrusts deadlocked in the different channels, the control reconfiguration strategy could be composed by the results of one engine or two engines deadlocked that we discussed before. The concrete analysis in detail is omitted temporarily here.

## 2.5 Stability Analysis

In the pitching channel for instance, from the analysis in the Appendix, the parameter $b_2^{\varphi} = m_z^{\alpha} q S_m l_k / J_z$ and its physics derivation is obtained obviously. Here, $m_z^{\alpha} = C_{y1}^{\alpha}(x_{\text{press}} - x_{\text{mass}})/l_k$ is called the Aerodynamic Moment Coefficient (or Static Stability Moment Coefficient), which presents the static stability of the vehicle by the distribution of the press center and mass center. We put $m_z^{\alpha}$ into the expression of $b_2^{\varphi}$ here, to find its implication of the stability of the vehicle.

$$b_2^{\varphi} = \frac{m_z^{\alpha} q S_m l_k}{J_z} = \frac{C_{y1}^{\alpha}(x_{\text{press}} - x_{\text{mass}}) q S_m}{J_z} \tag{2.29}$$

The following analysis is available.

**Lemma 1** *Assume the lift coefficient $C_{y1}^{\alpha}$, the character area $S_m$ and the moment of inertia $J_z$ are the positive constants. The velocity head $q = \frac{1}{2}\rho V_w^2 \geq 0$ with the atmospheric density $\rho > 0$.*

*Using a positive constant $K$ to indicate the product of the coefficients above:*

$$K = \frac{C_{y1}^{\alpha} q S_m}{J_z} \geq 0 \tag{2.30}$$

*Then, we have:*

$$b_2^{\varphi} = K(x_{\text{press}} - x_{\text{mass}}) \tag{2.31}$$

*While $b_2^{\varphi} > 0$, $x_{\text{press}} > x_{\text{mass}}$. In this way, the press center is at the lower place of the vehicle than the mass center. Then, the attack angle will be decreased autonomously by the aerodynamic moment without the control and the vehicle is asymptotic stable.*

*On the other hand, if $b_2^{\varphi} < 0$, $x_{\text{press}} < x_{\text{mass}}$. The press center is at the upper place of the vehicle than the mass center. Then, the vehicle is static unstable without control under the aerodynamic moment of force.*

Based on the Lemma 1, the sign of the system coefficient $b_2^{\varphi}$ denotes the inherent aerodynamic stability of the launch vehicle. The dynamic stability of the launch vehicle is studied from the comprehensive influences of aerodynamic, air dam, gravitational force, etc.

Considering the pitching channel for instance, the system has two input signal as the oscillating angle from the strap-on thrusts $\delta_{\text{strap-on}}^{\varphi}$ and core thrusts $\delta_{\text{core}}^{\varphi}$. Considering the relation of the input and output is $\Delta\varphi = G_1 \Delta\delta_{\text{strap-on}}^{\varphi} + G_2 \Delta\delta_{\text{core}}^{\varphi}$. The transfer functions $G_1$ and $G_2$ of the system are:

$$G_1 = \frac{\Delta\varphi}{\Delta\delta_{\text{strap-on}}^{\varphi}} = \frac{q_3 s^3 + q_2 s^2 + q_1 s + q_0}{s^3 + p_2 s^2 + p_1 s + p_0} \tag{2.32}$$

with the parameters:

$$\begin{aligned}
q_0 &= b_2^{\varphi} c_{3\text{strap-on}}^{\varphi} + (c_2^{\varphi} - c_1^{\varphi}) b_{3\text{strap-on}}^{\varphi} \\
q_1 &= -b_{3\text{strap-on}}^{\varphi} \\
q_2 &= b_{3\text{strap-on}}^{\prime\varphi} (c_2^{\varphi} - c_1^{\varphi}) + b_2^{\varphi} c_{3\text{strap-on}}^{\prime\varphi} \\
q_3 &= -b_{3\text{strap-on}}^{\prime\varphi} \\
p_0 &= -b_2^{\varphi} c_2^{\varphi} \\
p_1 &= b_2^{\varphi} + c_1^{\varphi} b_1^{\varphi} - b_1^{\varphi} c_2^{\varphi} \\
p_2 &= b_1^{\varphi} + c_1^{\varphi} - c_2^{\varphi}
\end{aligned}$$

and

$$G_2 = \frac{\Delta\varphi}{\Delta\delta_{\text{core}}^{\varphi}} = \frac{q_3 s^3 + q_2 s^2 + q_1 s + q_0}{s^3 + p_2 s^2 + p_1 s + p_0} \tag{2.33}$$

with the parameters:

$$\begin{aligned}
q_0 &= b_2^{\varphi} c_{3\text{core}}^{\varphi} + (c_2^{\varphi} - c_1^{\varphi}) b_{3\text{core}}^{\varphi} \\
q_1 &= -b_{3\text{core}}^{\varphi} \\
q_2 &= b_{3\text{core}}^{\prime\varphi} (c_2^{\varphi} - c_1^{\varphi}) + b_2^{\varphi} c_{3\text{core}}^{\prime\varphi} \\
q_3 &= -b_{3\text{core}}^{\prime\varphi} \\
p_0 &= -b_2^{\varphi} c_2^{\varphi} \\
p_1 &= b_2^{\varphi} + c_1^{\varphi} b_1^{\varphi} - b_1^{\varphi} c_2^{\varphi} \\
p_2 &= b_1^{\varphi} + c_1^{\varphi} - c_2^{\varphi}
\end{aligned}$$

Study the eigen-equation of the related transfer functions:

$$D(s) = s^3 + (b_1^{\varphi} + c_1^{\varphi} - c_2^{\varphi}) s^2 + (b_2^{\varphi} + c_1^{\varphi} b_1^{\varphi} - b_1^{\varphi} c_2^{\varphi}) s - b_2^{\varphi} c_2^{\varphi}$$

and the attitude stability of the system in the typical phase of flight.

### 2.5.1 Rocket Taking-Off

At this moment, the air damping coefficient $b_1^{\varphi} \approx 0$. The eigen-equation of the system can be simplified approximately as:

$$D(s) \approx s^3 + (c_1^{\varphi} - c_2^{\varphi}) s^2 + b_2^{\varphi} s - b_2^{\varphi} c_2^{\varphi}$$

Study the coefficients of the eigen-equation. The thrust and aerodynamic resistance related coefficient $c_1^{\varphi} = \frac{(2P_{\text{core}} + 4P_{\text{strap-on}})\cos\alpha_0 + C_y^{\alpha} q S_m}{mV}$ and the gravity-related coefficient $c_2^{\varphi} = \frac{g \sin\theta_0}{V}$.

Consider the discrepancy:

$$c_1^{\varphi} - c_2^{\varphi} = \frac{(2P_{\text{core}}+4P_{\text{strap-on}})\cos\alpha_0 + C_y^{\alpha} q S_m - mg\sin\theta_0}{mV} > 0$$

and the coefficient $c_2^{\varphi} > 0$, however, the other two coefficients $b_2^{\varphi}$ and $-b_2^{\varphi}c_2^{\varphi}$ cannot be positive at the same time. The eigen-equation will have positive root, and therefore, the system has unstable components, described as follow.

If $b_2^{\varphi} < 0$, the vehicle is static unstable by aerodynamic moment. Assume the eigen-equation can be transformed to following polynomial multiplication form.

$$D(s) = (s + c_1^{\varphi} - c_2^{\varphi})(s^2 + 2\xi\omega s + \omega^2)$$

in which, $\omega = \sqrt{-\frac{b_2^{\varphi}c_2^{\varphi}}{c_1^{\varphi}-c_2^{\varphi}}}$, $\xi\omega = \frac{b_2^{\varphi}c_1^{\varphi}}{2(c_1^{\varphi}-c_2^{\varphi})^2} < 0$.

Therefore, there is a pair of complex roots in the right half $s$ plane. The attitude motion is oscillating divergent.

If $b_2^{\varphi} > 0$, the vehicle is static stable. The eigen-equation can be decomposed as:

$$D(s) = (s + c_1^{\varphi} - c_2^{\varphi})\left[s - \frac{b_2^{\varphi}c_1^{\varphi}}{2(c_1^{\varphi}-c_2^{\varphi})^2} + \sqrt{\frac{b_2^{\varphi}c_2^{\varphi}}{c_1^{\varphi}-c_2^{\varphi}}}\right] \cdot \left[s + \frac{b_2^{\varphi}c_1^{\varphi}}{2(c_1^{\varphi}-c_2^{\varphi})^2} - \sqrt{\frac{b_2^{\varphi}c_2^{\varphi}}{c_1^{\varphi}-c_2^{\varphi}}}\right]$$

in which, $\frac{b_2^{\varphi}c_1^{\varphi}}{2(c_1^{\varphi}-c_2^{\varphi})^2} - \sqrt{\frac{b_2^{\varphi}c_2^{\varphi}}{c_1^{\varphi}-c_2^{\varphi}}} < 0$

Therefore, there will be a positive real root in the right half $s$ plane, and the attitude motion will be monotonic divergent.

### 2.5.2 With Maximum Aerodynamic Moment Coefficient $|m_z^{\alpha}|$

Since we have: $b_2^{\varphi} = \frac{m_z^{\alpha} q S_m l_k}{J_z}$, the coefficient $|b_2^{\varphi}|$ is maximum as well.

The eigen-equation is:

$$\begin{aligned} D(s) &= s^3 + (b_1^{\varphi} + c_1^{\varphi} - c_2^{\varphi})s^2 + (b_2^{\varphi} + c_1^{\varphi} - b_1^{\varphi}c_2^{\varphi})s - b_2^{\varphi}c_2^{\varphi} \\ &\approx s^3 + (b_1^{\varphi} - c_2^{\varphi})s^2 + (b_2^{\varphi} - b_1^{\varphi}c_2^{\varphi})s - b_2^{\varphi}c_2^{\varphi} \\ &\approx (s - c_2^{\varphi})(s^2 + b_1^{\varphi}s + b_2^{\varphi}) \end{aligned}$$

If $b_2^{\varphi} > 0$, vehicle is static stable.

$$s^2 + b_1^{\varphi}s + b_2^{\varphi} = s^2 + 2\xi\omega + \omega^2$$

in which $\omega = \sqrt{b_2^{\varphi}}$, $\xi\omega = \frac{b_1^{\varphi}}{2} > 0$.

Thus, the eigen-equation has a real root $s = c_2^{\varphi}$ in the right half $s$ plane. The attitude motion is monotonic divergent slowly because of the gravity.

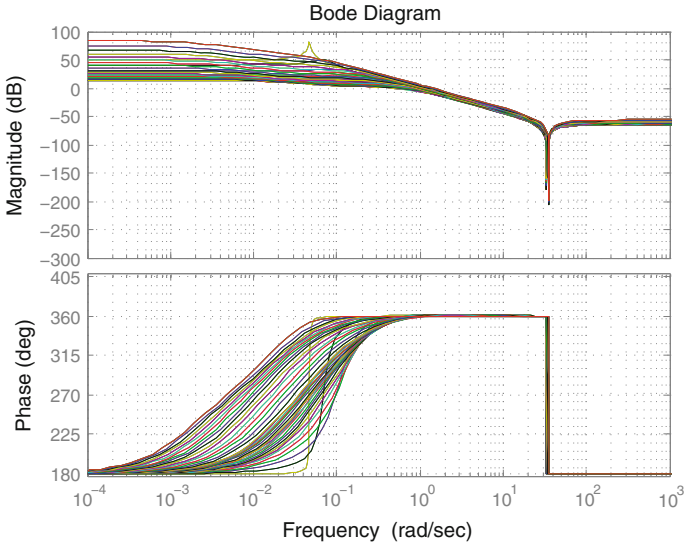


**Fig. 2.5** Bode diagram before correction

If $b_2^{\varphi} < 0$, vehicle is static unstable.

$$s^2 + b_1^{\varphi} s + b_2^{\varphi} = s^2 + 2\xi\omega + \omega^2 \approx \left(s - \sqrt{|b_2^{\varphi}|}\right)\left(s + \sqrt{|b_2^{\varphi}|}\right)$$

There are two real roots $s = c_2^{\varphi}$ and $s = \sqrt{|b_2^{\varphi}|}$ in the right half $s$ plane. The system will be divergent quickly by the effect of aerodynamic force.

### *2.5.3 First-Stage Engines Power-Off*

Since the air density is very slight at the hight that the first stage thrusts are power-off, the aerodynamic moment can be ignored and the coefficients $b_1^{\varphi}$ and $b_2^{\varphi}$ are negligible. The simplified eigen-equation is:

$$D(s) \approx s^3 + (c_1^{\varphi} - c_2^{\varphi})s^2 = s^2(s + c_1^{\varphi} - c_2^{\varphi})$$

There are a couple of poles $s = 0$ in the original point, and another single pole $s = -(c_1^{\varphi} - c_2^{\varphi}) < 0$ in the left half plane. The system is marginally stable, which will be divergent with the external disturbance.

We can draw the Bode diagram and the Nyquist curve to indicate the stability of the certain type of the vehicle in Figs. 2.5 and 2.6.

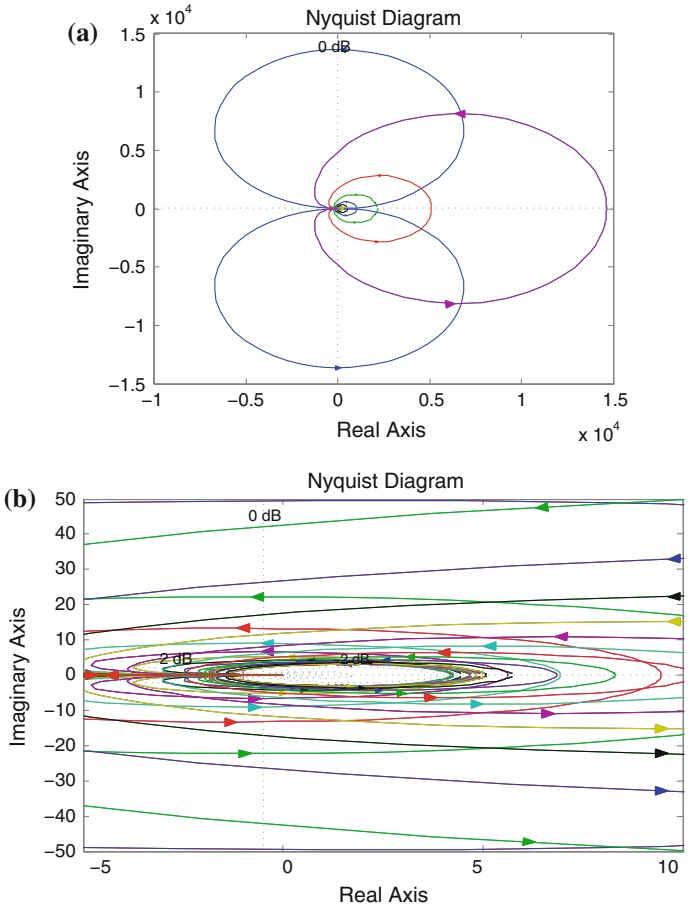


**Fig. 2.6** Nyquist curves before correction and partial enlargement at $(-1, 0)$

Obviously, the system is inherent unstable. Thus, an error feedback based attitude controller by the classic frequency correction method should be designed to stabilize the system. Then, we can plot the bode diagram to indicate the magnitude-phase characteristics of the corrected system (see Fig. 2.7), and the Nyquist curve after frequency-domain correction (see Fig. 2.8) as well.

Moreover, the step-response is proposed to investigate the static and dynamic property of the controller. Obviously, the system can be stabilized in 1.5 s and the overshoot is less than 20 % (see Fig. 2.9).

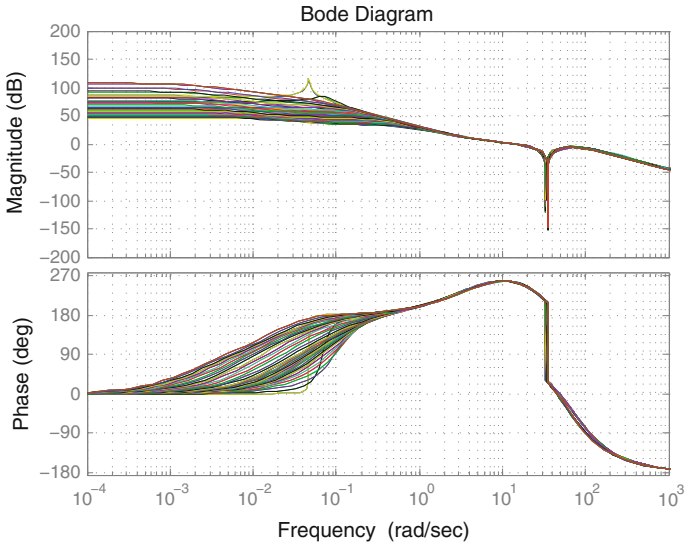


**Fig. 2.7** Bode diagram after correction

## 2.6 Reconfigurability Analysis

The above research is to find the proper compensation strategies to regulate the oscillating angles for control reconfiguration of the launch vehicle, when the thrusts are deadlocked at determined angles. However, for a physical system, the oscillation angle of the servomechanism is always bounded. Thus, in some limit cases, the above reconfiguration strategy cannot achieve the respected compensation because of its physics restriction. Therefore, in this section, rationally, the reconfigurability of the compensation strategy is studied under the certain numeral assumptions.

To simplify the discussion, the following assumption is proposed before the reconfigurability analysis:

**Assumption 6.1** *Consider a certain kind of the launch vehicle with:*

*(I) thrust power of the strap-on engines and core engines:* $N_s = N_c$*;*
*(II) proportion relation between the oscillating angle of strap-on and core engines: k=1;*
*(III) radius of the strap-on engine cluster circle and core engines cluster circle: R=3r.*

Based on the Assumption 6.1 above, we consider the situation that deadlock occurs on the strap-on thrust No. 2 for instance, so $\delta_6' = \tilde{\delta}_6$.

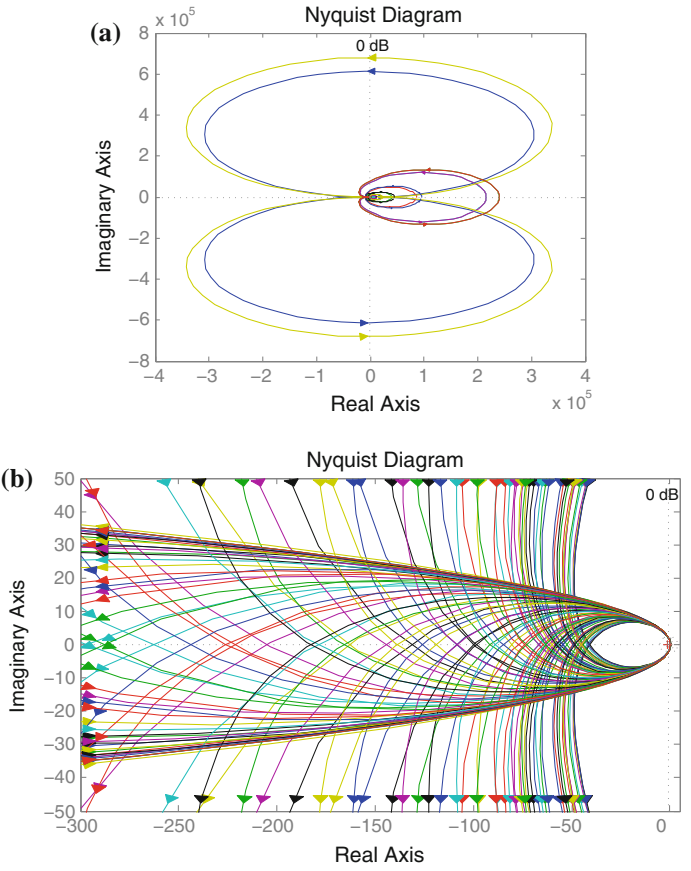


**Fig. 2.8** Nyquist curves after correction (**a**) and partial enlargement (**a**) at $(-1, 0)$

From the Eq. (2.18) and the assumptions, we have:

$$\begin{cases} \delta'_2 = \delta_2 - \frac{5}{3}\Delta\delta_6 \\ \delta'_4 = \delta_4 - \frac{1}{3}\Delta\delta_6 \\ \delta'_6 = \tilde{\delta}_6 = \delta_6 + \Delta\delta_6 \\ \delta'_8 = \delta_8 - \frac{1}{3}\Delta\delta_6 \end{cases} \tag{2.34}$$

Give the bounds of the oscillating angle of both strap-on and core engines are:

$$-\overline{\delta} \leq \delta_i \leq \overline{\delta} \quad (\text{with } \ i = 1, 2, 3, \ldots, 8). \tag{2.35}$$

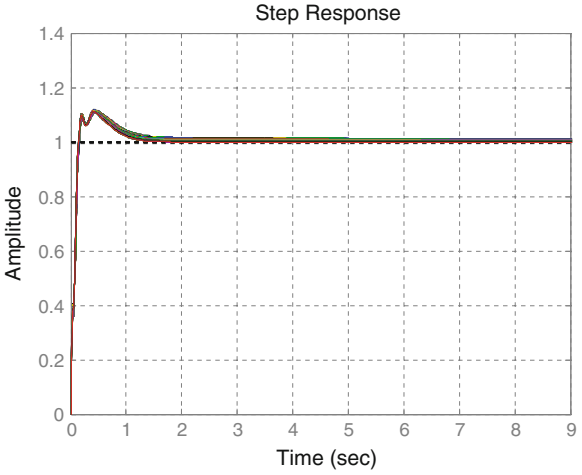


**Fig. 2.9** Step-response curves of the system

Theoretically, the maximum disparity of the angle $\Delta\delta_i = \delta_i - \delta_i'$ satisfies:

$$-2\overline{\delta} \leq \Delta\delta_i \leq 2\overline{\delta} \tag{2.36}$$

Substitute the disparity between $\delta_2$ and $\delta_2'$ in Eq. (2.34) by Eq. (2.36), with $i = 2, 4, 8$.

$$\begin{cases} -2\overline{\delta} \leq \frac{1}{3}\Delta\delta_6 \leq 2\overline{\delta} \\ -2\overline{\delta} \leq \frac{5}{3}\Delta\delta_6 \leq 2\overline{\delta} \\ -2\overline{\delta} \leq \frac{1}{3}\Delta\delta_6 \leq 2\overline{\delta} \end{cases} \tag{2.37}$$

and then we have:

$$-1.2\overline{\delta} \leq \Delta\delta_6 \leq 1.2\overline{\delta} \tag{2.38}$$

Thus, if the disparity between the deadlocked angle of the failed thrust and its required angle is bigger than $|1.2\overline{\delta}|$, the reconfiguration strategies are unavailable for the control action compensation.

On the other hand, if the disparity angle of the failed actuator is within the interval of $\left[-1.2\overline{\delta}, 1.2\overline{\delta}\right]$, because the oscillation angle satisfies the inequality (2.35), the reconfigurable interval of the deadlocked angle should be within the range of $\left[-0.2\overline{\delta}, 0.2\overline{\delta}\right]$ to guarantee the reliability of the compensation.

So, the reconfigurability condition of the oscillation angle $\delta_6'$ deadlock is:

$$-0.2\overline{\delta} \leq \delta_6' \leq 0.2\overline{\delta} \tag{2.39}$$

Because of the symmetry, the same result will be obtained when one of other oscillation engines is deadlocked.

Second, the situation of two thrusts in the certain channel deadlocked at the same time is considered. Supposing that the booster thrusts strap-on2 and strap-on4 are deadlocked corresponding to the oscillating angles $\delta_6$ and $\delta_8$, the Eq. (2.22) can be transformed based on the Assumption 6.1:

$$\begin{cases} \delta'_2 = \delta_2 - 2\Delta\delta_6 - \Delta\delta_8 \\ \delta'_4 = \delta_4 - \Delta\delta_6 - 2\Delta\delta_8 \end{cases} \tag{2.40}$$

Then, a set of inequalities is available from Eq. (2.36):

$$\begin{cases} -2\bar{\delta} \le 2\Delta\delta_6 + \Delta\delta_8 \le 2\bar{\delta} \\ -2\bar{\delta} \le \Delta\delta_6 + 2\Delta\delta_8 \le 2\bar{\delta} \end{cases} \tag{2.41}$$

Therefore, from the inequalities (2.41) above, the reconfigurability conditions for the composed oscillating angle $\delta_6$ and $\delta_8$ when two thrusts strap-on2 and strap-on4 are failed simultaneously.

$$-\tfrac{4}{3}\bar{\delta} \le \Delta\delta_6 + \Delta\delta_8 \le \tfrac{4}{3}\bar{\delta} \tag{2.42}$$

Obviously, the control operation can only be reconfigured when the error of the composed oscillating angle is not bigger than $\frac{4}{3}\bar{\delta}$. Thus, to guarantee the control reconfigurability of the vehicle, the failed thrusts should not be deadlocked at the fringe place. For example, if $\Delta\delta_6 = \Delta\delta_8 = \bar{\delta}$, the inequalities (2.41) are unsubstantiated.

Similarly, we can derive the same results when thrusts strap-on2 and core2 are deadlocked, and thrusts strap-on2 and core4 are deadlocked.

## 2.7 Simulation Result

We have studied a launch vehicle system which can be described by the dynamic model in Eqs. (2.5), (2.6) and (2.7) to demonstrate the performance of the control reconfiguration strategies while a helm of an engine is deadlocked.

First of all, an attitude controller is designed to stabilize the program angle tracking control. In this structure, the control commands produced from the controller are the equivalent oscillating angles: $\delta_\varphi$, $\delta_\psi$ and $\delta_\gamma$. However, the physical actuators are the oscillating angles of the helms of four strap-on thrusts and two core thrusts: $\delta_1$ to $\delta_8$ in Fig. 2.3. Thus, an angle composing and decomposing block of the oscillating engines is required between the controller and launch vehicle to transform the equivalent angles to the oscillating angles of the physical actuators. In this way, when the deadlocking fault is occurred, the above control reconfiguration strategy will be

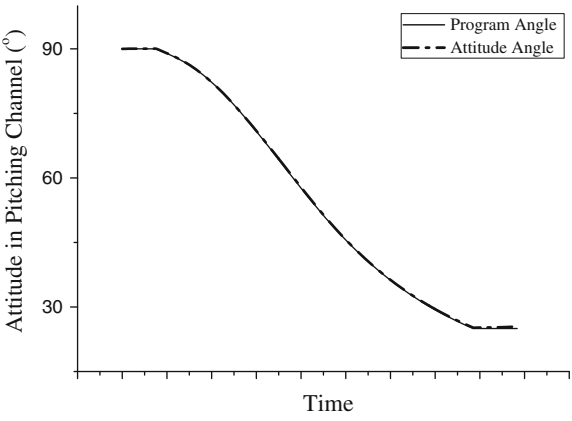


**Fig. 2.10** Attitude control in pitching channel

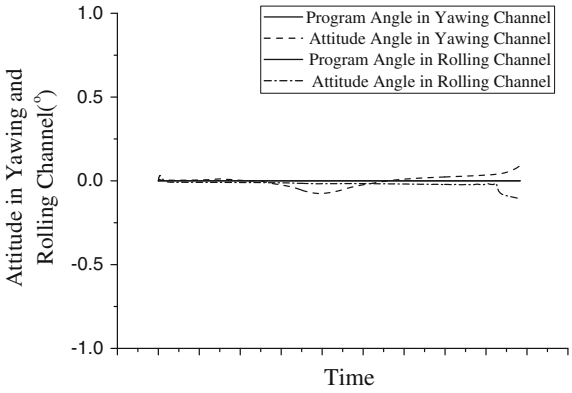


**Fig. 2.11** Attitude control in yawing and rolling channel

operated to reconfigure the control efforts of the gimballed thrust that still works. Furthermore, a disturbance compensation part is developed to decrease the effect of the general disturbance (such as wind and air damping) and perturbation (such as model uncertainties). The attitude control and fault-tolerance structure in our simulation is shown in Fig. 2.4.

Then, assuming the motion of the launch vehicle satisfies the following assumptions: the vehicle is launched vertically and then turns to about 30° in pitching channel in the certain program turning time period, and meanwhile, other two channels of Yawing and Rolling should maintain 0° attitude angle under the influence of inside and outside disturbances.

The curves in Figs. 2.10 and 2.11 compare the program angles and the flight attitude angles with disturbance by using the designed attitude controller, in which the solid curves denote the program angles in three channels given by the guidance process and the dash curves and dot dash curves are the flight attitude angles from simulation. Thereby, although the disturbance can cause some turbulence to the

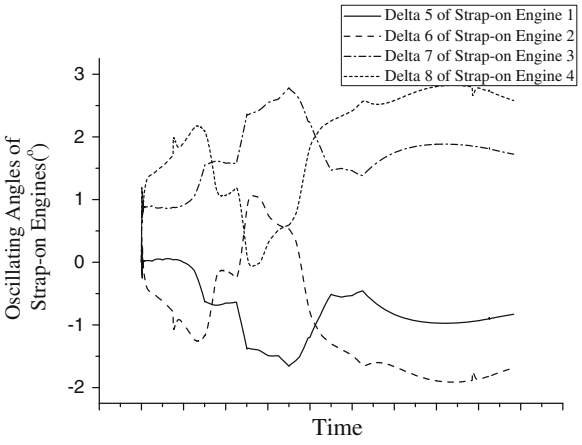


**Fig. 2.12** Curve of the oscillating angles of strap-on engines without deadlocked engine

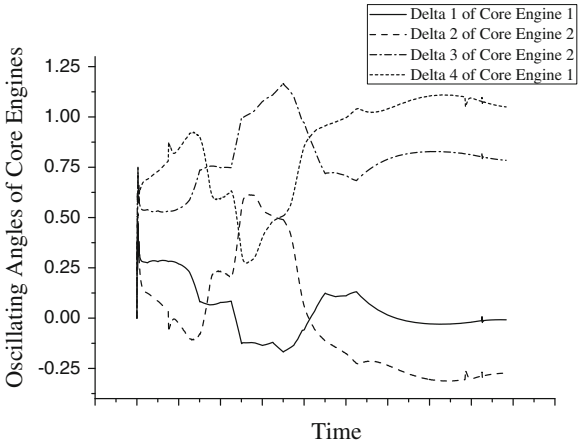


**Fig. 2.13** Curves of the oscillating angles of core thrusts without deadlocked thrust

rocket flight, the attitudes of the vehicle can follow the program angles precisely with the errors of about $\pm 0.1°$.

Based on the attitude controller, we add the control reconfiguration strategies into the system to study the fault-tolerance ability of the system. Here we assume that the fault occurs randomly, and then stays at a certain angle. In order to test the command angle of each engine, we give the dynamic tracking curves of the oscillating angles of both strap-on and core engines with and without the deadlocked fault.

The command angles of oscillation without the deadlocked engine are shown in Figs. 2.12 and 2.13.

It is obvious that the command angles of oscillating angles of each engine are in couple in order to counteract the effect to the rolling channel. Moreover, the command

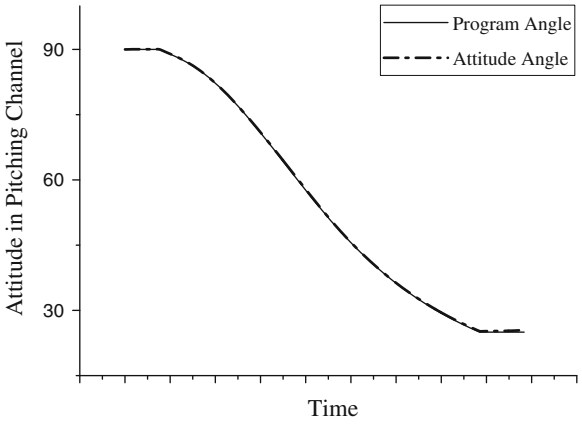


**Fig. 2.14** The pitching control results with one deadlocked thrust

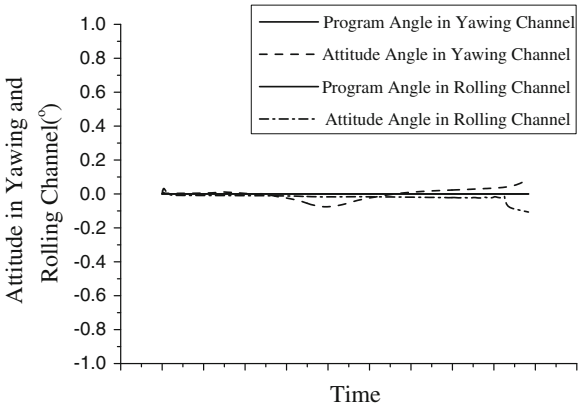


**Fig. 2.15** The yawing and rolling control result with one deadlocked thrust

angles of the thrusts are all less than 3°, which satisfies the physical limitation 10° of the helm mechanism.

After that, considering the faulty situation, assuming that the strap-on thrust II is deadlocked randomly, we choose a random deadlocked time point and simulate the situation that one strap-on2 is deadlocked. First, the attitude control results with one damaged thrust is shown in Figs. 2.14 and 2.15, comparing with the original control performance in Figs. 2.10 and 2.11. We can see that the attitude angles in pitching, yawing, and rolling channel can track the program angles accurately with one thrust deadlocked.

Then, we displace the command angles of both strap-on and core thrusts in Figs. 2.16 and 2.17. In Fig. 2.16, the position feedback of the servomechanism shows

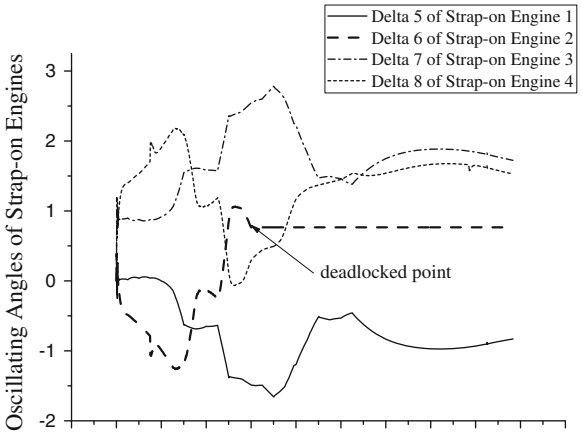


**Fig. 2.16** Curve of the oscillating angles of strap-on thrusts with one deadlocked thrust

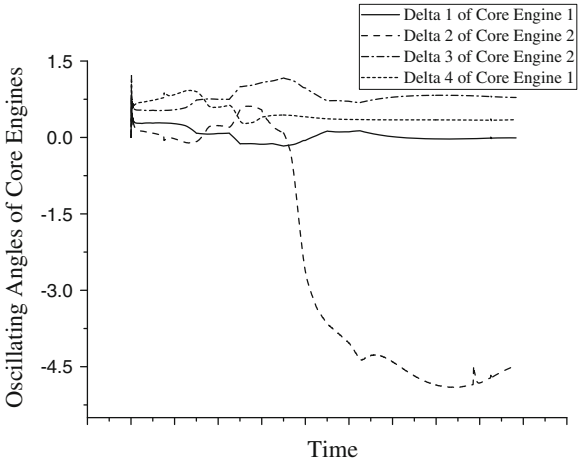


**Fig. 2.17** Curves of the oscillating angles of core thrusts with one deadlocked thrust

that the strap-on thrust II is deadlocked at about $\delta_6 = 0.8°$. Then its corresponding angle $\delta_8$ (Delta 8) affords more to control the attitude to counteract the deadlocked angle.

Similarly, the oscillating angles of the core thrusts contribute in the fault compensation as well. The oscillating angle $\delta_2$ (Delta 2) of core thrust 2 and its corresponding angle $\delta_4$ (Delta 4) in the pitching channel, are changing simultaneously while $\delta_6$ (Delta 6) is deadlocked. Because of the symmetry between $\delta_2$ and $\delta_6$, $\delta_2$ will change more than the other thrusts.

## 2.8 Conclusion

A control reconfiguration FTC strategy is introduced in this chapter for the new generation "CZ" launch vehicle in China under the no rolling movement assumption. The attitude controller is designed by the frequency method based on its dynamic model to achieve the stable movement of the vehicle without fault. From the analysis of the core and strap-on thrusts, which involve in the control in our new generation vehicle, the redundancy in control of the thrusts provides the additional manipulation capability to the vehicle with damaged thrusts. After that, the reconfiguration strategies are proposed for several conventional scenarios of thrusts deadlocked, which is real-time operated but without increasing the robustness of the system. It can be improved in the attitude controller design in our further work. However, we find that the vehicle motion is unable to be recovered in some extreme situations. So, the reconfigurability analysis is given to obtain the recoverable conditions of the vehicle, which is very harsh when more than one thrust is deadlocked. Finally, the chapter gives a set of simulation results, including the real-time attitude tracking control in three channels and the oscillating angles of all thrusts, with and without the fault occurred. It is illustrated that, the reconfiguration strategy has achieved the regulation of the control operation between the failed thrusts and normal thrusts to maintain the adequate manipulation in attitude control.

**Acknowledgments** This work is supported in part by the National Nature Science Foundation of China No 61203081 and 61174079, the Doctoral Fund of Ministry of Education of China NO.20120142120091, and the Precision manufacturing technology and equipment for metal parts NO.2012DFG70640.

## Appendix: Dynamic Modeling Analysis

From the dynamics of the motion of the mass center and the rotation around the mass center in three axis directions $x$, $y$, and $z$.

$$\begin{cases} \delta m \frac{\mathrm{d}\mathbf{V}}{\mathrm{d}t} = \sum \mathbf{F}_x = \mathbf{F}_{Gx} + \mathbf{F}_{Px} + \mathbf{F}_{Ax} + \mathbf{F}_{Cx} + \mathbf{F}_{Ex} + \mathbf{F}_x \\ \delta m \mathbf{V} \frac{\mathrm{d}\theta}{\mathrm{d}t} = \sum \mathbf{F}_y = \mathbf{F}_{Gy} + \mathbf{F}_{Py} + \mathbf{F}_{Ay} + \mathbf{F}_{Cy} + \mathbf{F}_{Ey} + \mathbf{F}_y \\ -\delta m \mathbf{V} \frac{\mathrm{d}\sigma}{\mathrm{d}t} = \sum \mathbf{F}_z = \mathbf{F}_{Gz} + \mathbf{F}_{Pz} + \mathbf{F}_{Az} + \mathbf{F}_{Cz} + \mathbf{F}_{Ez} + \mathbf{F}_z \\ \delta J_x \frac{\mathrm{d}\omega_x}{\mathrm{d}t} + (\delta J_z - \delta J_y)\omega_z\omega_y = \sum \mathbf{M}_x = \mathbf{M}_{Ax} + \mathbf{M}_{Cx} + \mathbf{M}_{Ex} + \mathbf{M}_x \\ \delta J_y \frac{\mathrm{d}\omega_y}{\mathrm{d}t} + (\delta J_x - \delta J_z)\omega_x\omega_z = \sum \mathbf{M}_y = \mathbf{M}_{Ay} + \mathbf{M}_{Cy} + \mathbf{M}_{Ey} + \mathbf{M}_y \\ \delta J_z \frac{\mathrm{d}\omega_z}{\mathrm{d}t} + (\delta J_y - \delta J_x)\omega_y\omega_x = \sum \mathbf{M}_z = \mathbf{M}_{Az} + \mathbf{M}_{Cz} + \mathbf{M}_{Ez} + \mathbf{M}_z \end{cases}$$

We consider the motion in the pitching channel of flight period for instance.

$$\begin{cases} \delta m \mathbf{V} \frac{\mathrm{d}\theta}{\mathrm{d}t} = \mathbf{F}_{Gy} + \mathbf{F}_{Py} + \mathbf{F}_{Ay} + \mathbf{F}_{Cy} + \mathbf{F}_{Ey} + \mathbf{F}_y \\ \delta J_z \frac{\mathrm{d}\omega_z}{\mathrm{d}t} + (\delta J_y - \delta J_x)\omega_y\omega_x = \mathbf{M}_{Az} + \mathbf{M}_{Cz} + \mathbf{M}_{Ez} + \mathbf{M}_z \end{cases}$$

The controlling forces and moments are $\mathbf{F}_C = \mathbf{F}_C^{\text{core}} + \mathbf{F}_C^{\text{strap-on}}$, $\mathbf{M}_C = \mathbf{M}_C^{\text{core}} + \mathbf{M}_C^{\text{strap-on}}$, and the inertial forces and moments of the gimballed thrusts are: $\mathbf{F}_E = \mathbf{F}_E^{\text{core}} + \mathbf{F}_E^{\text{strap-on}}$, $\mathbf{M}_E = \mathbf{M}_E^{\text{core}} + \mathbf{M}_E^{\text{strap-on}}$.

Consider the dynamics of the general launch vehicle without vibration and shaking elements can be symbolized separately by the simultaneous equations as follow in three attitudes [24]:

From the dynamic equation of the flight.

$$\begin{aligned}
\mathbf{F}_{Gy} &= -mg\cos\theta_0 \\
\mathbf{F}_{Py} &= \sum_{\text{core\&strap-on}} P_i \cos\beta \sin\alpha \\
&\overset{\beta\to 0}{\approx} (2P_{\text{core}} + 4P_{\text{strap-on}})\sin\alpha \\
\mathbf{F}_{Ay} &= C_y^{\alpha} q S_m (\alpha + \alpha_w) \\
\mathbf{F}_{Cy}^{\text{core}} &= 2P_{\text{core}}\delta_{\varphi}^{\text{core}} \\
\mathbf{F}_{Cy}^{\text{strap-on}} &= 2P_{\text{strap-on}}\delta_{\varphi}^{\text{strap-on}} \\
\mathbf{F}_{Cy} &= \mathbf{F}_{Cy}^{\text{core}} + \mathbf{F}_{Cy}^{\text{strap-on}} \\
&= 2P_{\text{core}}\delta_{\varphi}^{\text{core}} + 2P_{\text{strap-on}}\delta_{\varphi}^{\text{strap-on}}
\end{aligned}$$

$$\begin{aligned}
\mathbf{F}_{Ey}^{\text{core}} &= m_R l_R \ddot{\delta}_{\varphi}^{\text{core}} - m_R \dot{W}_x \delta_{\varphi}^{\text{core}} \\
\mathbf{F}_{Ey}^{\text{strap-on}} &= m_R l_R \ddot{\delta}_{\varphi}^{\text{strap-on}} - m_R \dot{W}_x \delta_{\varphi}^{\text{strap-on}} \\
\mathbf{F}_{Ey} &= \mathbf{F}_{Ey}^{\text{core}} + \mathbf{F}_{Ey}^{\text{strap-on}} \\
&= m_R^{\text{core}} l_R^{\text{core}} \ddot{\delta}_{\varphi}^{\text{core}} - m_R^{\text{core}} \dot{W}_x \delta_{\varphi}^{\text{core}} + m_R^{\text{strap-on}} l_R^{\text{strap-on}} \ddot{\delta}_{\varphi}^{\text{strap-on}} \\
&\quad - m_R^{\text{strap-on}} \dot{W}_x \delta_{\varphi}^{\text{strap-on}}
\end{aligned}$$

About the moment:

$$\begin{aligned}
\mathbf{M}_{Asz} &= -F_{Ay}(x_{\text{press}} - x_{\text{mass}}) \\
&= -C_y^{\alpha} q S_m (\alpha + \alpha_w)(x_{\text{press}} - x_{\text{mass}}) \\
&= -m_z^{\alpha} q S_m l_k (\alpha + \alpha_w)
\end{aligned}$$

with the dimensionless Steady Stability Moment Coefficient: $m_z^{\alpha} = C_y^{\alpha}(x_{\text{press}} - x_{\text{mass}})/l_k$, which is called Aerodynamic Moment Coefficient as well. Here n, $x_{\text{press}}$ and $x_{\text{mass}}$ are the distance from the theory top of the vehicle to the aerodynamic press center and to the mass center,
autoedited1, respectively.

$$\mathbf{M}_{Adz} = -\frac{m_{dz}^{\omega} q S_m l_k^2 \omega_z}{V} = -\frac{m_{dz}^{\omega} q S_m l_k^2}{V}\dot{\varphi}$$

is the damping moment from atmospheric.

Thus,

$$\begin{aligned}
\mathbf{M}_{Az} &= \mathbf{M}_{Asz} + \mathbf{M}_{Adz} \\
&= -m_z^{\alpha} q S_m l_k(\alpha + \alpha_w) - \frac{m_{dz}^{\omega} q S_m l_k^2}{V}\dot{\varphi} \\
\mathbf{M}_{Cz}^{\text{core}} &= -\mathbf{F}_{Cy}^{\text{core}} \rho_C \\
&= -2P_{\text{core}}\delta_{\varphi}^{\text{core}} \rho_C \\
\mathbf{M}_{Cz}^{\text{strap-on}} &= -\mathbf{F}_{Cz}^{\text{strap-on}} \rho_C \\
&= -2P_{\text{strap-on}}\delta_{\varphi}^{\text{strap-on}} \rho_C \\
\mathbf{M}_{Cz} &= \mathbf{M}_{Cz}^{\text{core}} + \mathbf{M}_{Cz}^{\text{strap-on}} \\
&= -2P_{\text{core}}\delta_{\varphi}^{\text{core}} \rho_C - 2P_{\text{strap-on}}\delta_{\varphi}^{\text{strap-on}} \rho_C
\end{aligned}$$

$$\begin{aligned}
\mathbf{M}_{Ez}^{\text{core}} &= -J_R^{\text{core}}\ddot{\delta}_{\varphi}^{\text{core}} - m_R^{\text{core}} l_R^{\text{core}} \rho_C \ddot{\delta}_{\varphi}^{\text{core}} - m_R^{\text{core}} \dot{W}_x l_R^{\text{core}} \delta_{\varphi}^{\text{core}} \\
\mathbf{M}_{Ez}^{\text{strap-on}} &= -J_R^{\text{strap-on}}\ddot{\delta}_{\varphi}^{\text{strap-on}} - m_R^{\text{strap-on}} l_R^{\text{strap-on}} \rho_C \ddot{\delta}_{\varphi}^{\text{strap-on}} \\
&\quad - m_R^{\text{strap-on}} \dot{W}_x l_R^{\text{strap-on}} \delta_{\varphi}^{\text{strap-on}}
\end{aligned}$$

$$\begin{aligned}
\mathbf{M}_{Ez} &= \mathbf{M}_{Ez}^{\text{core}} + \mathbf{M}_{Ez}^{\text{strap-on}} \\
&= -J_R^{\text{core}}\ddot{\delta}_{\varphi}^{\text{core}} - m_R^{\text{core}} l_R^{\text{core}} \rho_C \ddot{\delta}_{\varphi}^{\text{core}} - m_R^{\text{core}} \dot{W}_x l_R^{\text{core}} \delta_{\varphi}^{\text{core}} - J_R^{\text{strap-on}}\ddot{\delta}_{\varphi}^{\text{strap-on}} \\
&\quad - m_R^{\text{strap-on}} l_R^{\text{strap-on}} \rho_C \ddot{\delta}_{\varphi}^{\text{strap-on}} - m_R^{\text{strap-on}} \dot{W}_x l_R^{\text{strap-on}} \delta_{\varphi}^{\text{strap-on}}
\end{aligned}$$

First, the ideal situation without disturbances is considered to form its equilibrium equation based on Newton's second law in the pitching channel.

$$\begin{aligned}
mV\dot{\theta}_0 &= -mg\cos\theta_0 + (2P_{\text{core}} + 4P_{\text{strap-on}})\sin\alpha_0 + C_y^{\alpha} q S_m \alpha_0 \\
&\quad + (2P_{\text{core}}\delta_{\varphi 0}^{\text{core}} + 2P_{\text{strap-on}}\delta_{\varphi 0}^{\text{strap-on}}) + (m_R^{\text{core}} l_R^{\text{core}} \ddot{\delta}_{\varphi 0}^{\text{core}} - m_R^{\text{core}} \dot{W}_x \delta_{\varphi 0}^{\text{core}} \\
&\quad + m_R^{\text{strap-on}} l_R^{\text{strap-on}} \ddot{\delta}_{\varphi 0}^{\text{strap-on}} - m_R^{\text{strap-on}} \dot{W}_x \delta_{\varphi 0}^{\text{strap-on}}) \\
&= -mg\cos\theta_0 + (2P_{\text{core}} + 4P_{\text{strap-on}})\sin\alpha_0 + C_y^{\alpha} q S_m \alpha_0 + (2P_{\text{core}} - m_R^{\text{core}} \dot{W}_x)\delta_{\varphi 0}^{\text{core}} \\
&\quad + (2P_{\text{strap-on}} - m_R^{\text{strap-on}} \dot{W}_{x1})\delta_{\varphi 0}^{\text{strap-on}} + m_R^{\text{core}} l_R^{\text{core}} \ddot{\delta}_{\varphi 0}^{\text{core}} + m_R^{\text{strap-on}} l_R^{\text{strap-on}} \ddot{\delta}_{\varphi 0}^{\text{strap-on}}
\end{aligned}$$

Then, study the practical system with deviation of the Euler angles of the vehicle: $\Delta\theta$ and $\Delta\alpha$.

$$
\begin{aligned}
mV(\dot{\theta}_0+\Delta\dot{\theta}) = & -mg\cos(\theta_0+\Delta\theta)+(2P_{\text{core}}+4P_{\text{strap-on}})\sin(\alpha_0+\Delta\alpha)\\
& +C_y^{\alpha}qS_m(\alpha_0+\Delta\alpha+\alpha_w)+(2P_{\text{core}}-m_R^{\text{core}}\dot{W}_x)(\delta_{\varphi 0}^{\text{core}}+\delta_{\varphi}^{\text{core}})\\
& +(2P_{\text{strap-on}}-m_R^{\text{strap-on}}\dot{W}_x)\cdot(\delta_{\varphi 0}^{\text{strap-on}}+\delta_{\varphi}^{\text{strap-on}})+m_R^{\text{core}}l_R^{\text{core}}\\
& \cdot(\ddot{\delta}_{\varphi 0}^{\text{core}}+\ddot{\delta}_{\varphi}^{\text{core}})+m_R^{\text{strap-on}}l_R^{\text{strap-on}}\cdot(\ddot{\delta}_{\varphi 0}^{\text{strap-on}}+\ddot{\delta}_{\varphi}^{\text{strap-on}})+F_y\\
& \overset{\substack{\Delta\theta\to 0\\ \Delta\alpha\to 0}}{\approx} -mg(\cos\theta_0-\sin\theta_0\Delta\theta)+(2P_{\text{core}}+4P_{\text{strap-on}})(\sin\alpha_0+\cos\alpha_0\Delta\alpha)\\
& +C_y^{\alpha}qS_m(\alpha_0+\Delta\alpha)+(2P_{\text{core}}-m_R^{\text{core}}\dot{W}_x)(\delta_{\varphi 0}^{\text{core}}+\delta_{\varphi}^{\text{core}})\\
& +(2P_{\text{strap-on}}-m_R^{\text{strap-on}}\dot{W}_x)(\delta_{\varphi 0}^{\text{strap-on}}+\delta_{\varphi}^{\text{strap-on}})+m_R^{\text{core}}l_R^{\text{core}}(\ddot{\delta}_{\varphi 0}^{\text{core}}\\
& +\ddot{\delta}_{\varphi}^{\text{core}})+m_R^{\text{strap-on}}l_R^{\text{strap-on}}(\ddot{\delta}_{\varphi 0}^{\text{strap-on}}+\ddot{\delta}_{\varphi}^{\text{strap-on}})+C_y^{\alpha}qS_m\alpha_w+F_y
\end{aligned}
$$

$$
\begin{aligned}
mV\Delta\dot{\theta} = & mg\sin\theta_0\Delta\theta+(2P_{\text{core}}+4P_{\text{strap-on}})\cdot\cos\alpha_0\Delta\alpha+C_y^{\alpha}qS_m\Delta\alpha+(2P_{\text{core}}\\
& -m_R^{\text{core}}\dot{W}_x)\delta_{\varphi}^{\text{core}}+(2P_{\text{strap-on}}-m_R^{\text{strap-on}}\dot{W}_x)\delta_{\varphi}^{\text{strap-on}}\\
& +m_R^{\text{core}}l_R^{\text{core}}\ddot{\delta}_{\varphi}^{\text{core}}+m_R^{\text{strap-on}}l_R^{\text{strap-on}}\cdot\ddot{\delta}_{\varphi}^{\text{strap-on}}+C_y^{\alpha}qS_m\alpha_w+F_y\\
= & \left[(2P_{\text{core}}+4P_{\text{strap-on}})\cos\alpha_0+C_y^{\alpha}qS_m\right]\cdot\Delta\alpha+mg\sin\theta_0\Delta\theta+(2P_{\text{core}}\\
& -m_R^{\text{core}}\dot{W}_x)\cdot\delta_{\varphi}^{\text{core}}+m_R^{\text{core}}l_R^{\text{core}}\ddot{\delta}_{\varphi}^{\text{core}}+(2P_{\text{strap-on}}-m_R^{\text{strap-on}}\dot{W}_x)\delta_{\varphi}^{\text{strap-on}}\\
& +m_R^{\text{strap-on}}l_R^{\text{strap-on}}\ddot{\delta}_{\varphi}^{\text{strap-on}}+C_y^{\alpha}qS_m\alpha_w+F_y
\end{aligned}
$$

$$
\begin{aligned}
\Delta\dot{\theta} = & \frac{(2P_{\text{core}}+4P_{\text{strap-on}})\cos\alpha_0+C_y^{\alpha}qS_m}{mV}\Delta\alpha+\frac{g\sin\theta_0}{V}\Delta\theta+\frac{2P_{\text{core}}-m_R^{\text{core}}\dot{W}_x}{mV}\delta_{\varphi}^{\text{core}}\\
& +\frac{m_R^{\text{core}}l_R^{\text{core}}}{mV}\ddot{\delta}_{\varphi}^{\text{core}}+\frac{2P_{\text{strap-on}}-m_R^{\text{strap-on}}\dot{W}_x}{mV}\delta_{\varphi}^{\text{strap-on}}+\frac{m_R^{\text{strap-on}}l_R^{\text{strap-on}}}{mV}\ddot{\delta}_{\varphi}^{\text{strap-on}}\\
& +\frac{C_y^{\alpha}qS_m}{mV}\alpha_w+\frac{F_y}{mV}\\
= & c_1^{\varphi}\Delta\alpha+c_2^{\varphi}\Delta\theta+c_{3\text{core}}^{\varphi}\delta_{\varphi}^{\text{core}}+c_{3\text{core}}^{\prime\varphi}\ddot{\delta}_{\varphi}^{\text{core}}+c_{3\text{strap-on}}^{\varphi}\delta_{\varphi}^{\text{strap-on}}\\
& +c_{3\text{strap-on}}^{\prime\varphi}\ddot{\delta}_{\varphi}^{\text{strap-on}}+c_1^{\prime\varphi}\alpha_w+\overline{F}_{yc}
\end{aligned}
$$

In which, the coefficients are:

$$
\begin{aligned}
c_1^{\varphi} &= \frac{(2P_{\text{core}}+4P_{\text{strap-on}})\cos\alpha_0+C_y^{\alpha}qS_m}{mV}\\
c_2^{\varphi} &= \frac{g\sin\theta_0}{V}\\
c_{3\text{core}}^{\varphi} &= \frac{2P_{\text{core}}-m_R^{\text{core}}\dot{W}_{x1}}{mV}\\
c_{3\text{core}}^{\prime\varphi} &= \frac{m_R^{\text{core}}l_R^{\text{core}}}{mV}\\
c_{3\text{strap-on}}^{\varphi} &= \frac{2P_{\text{strap-on}}-m_R^{\text{strap-on}}\dot{W}_{x1}}{mV}
\end{aligned}
$$

$$c'^{\varphi}_{3\text{strap-on}} = \frac{m_R^{\text{strap-on}} l_R^{\text{strap-on}}}{mV}$$
$$c'^{\varphi}_{1} = \frac{C_y^{\alpha} q S_m}{mV}$$
$$\overline{F}_{yc} = \frac{F_y}{mV}$$

Similarly, from the

$$\begin{aligned}
&J_z(\ddot{\varphi}_0 + \Delta\ddot{\varphi}) + (J_y - J_x)(\dot{\gamma} - \dot{\varphi}_0\psi)(\dot{\psi} + \dot{\varphi}_0\gamma) \\
&= -m_z^{\alpha} q S_m l_k(\alpha_0 + \Delta\alpha + \alpha_w) - \frac{m_{dz}^{\omega} q S_m l_k^2}{V}(\dot{\varphi}_0 + \Delta\dot{\varphi}) - 2P_{\text{core}}\rho_C(\delta_{\varphi 0}^{\text{core}} + \delta_{\varphi}^{\text{core}}) \\
&-2P_{\text{strap-on}}\rho_C(\delta_{\varphi 0}^{\text{strap-on}} + \delta_{\varphi}^{\text{strap-on}}) - J_R^{\text{core}}(\ddot{\delta}_{\varphi 0}^{\text{core}} + \ddot{\delta}_{\varphi}^{\text{core}}) - m_R^{\text{core}} l_R^{\text{core}} \rho_C(\ddot{\delta}_{\varphi 0}^{\text{core}} + \ddot{\delta}_{\varphi}^{\text{core}}) \\
&-m_R^{\text{core}} \dot{W}_x l_R^{\text{core}}(\delta_{\varphi 0}^{\text{core}} + \delta_{\varphi}^{\text{core}}) - J_R^{\text{strap-on}}(\ddot{\delta}_{\varphi 0}^{\text{strap-on}} + \ddot{\delta}_{\varphi}^{\text{strap-on}}) - m_R^{\text{strap-on}} l_R^{\text{strap-on}} \\
&\cdot\rho_C(\ddot{\delta}_{\varphi 0}^{\text{strap-on}} + \ddot{\delta}_{\varphi}^{\text{strap-on}}) - m_R^{\text{strap-on}} \dot{W}_x l_R^{\text{strap-on}}(\delta_{\varphi 0}^{\text{strap-on}} + \delta_{\varphi}^{\text{strap-on}}) + M_z
\end{aligned}$$

$$\begin{aligned}
&= -m_z^{\alpha} q S_m l_k(\alpha_0 + \Delta\alpha) - \tfrac{m_{dz}^{\omega} q S_m l_k^2}{V}(\dot{\varphi}_0 + \Delta\dot{\varphi}) - (2P_{\text{core}}\rho_C + m_R^{\text{core}} \dot{W}_x l_R^{\text{core}})(\delta_{\varphi 0}^{\text{core}} + \delta_{\varphi}^{\text{core}}) \\
&-(2P_{\text{strap-on}}\rho_C + m_R^{\text{strap-on}} \dot{W}_x l_R^{\text{strap-on}})(\delta_{\varphi 0}^{\text{strap-on}} + \delta_{\varphi}^{\text{strap-on}}) - (J_R^{\text{core}} + m_R^{\text{core}} l_R^{\text{core}} \rho_C) \\
&\cdot(\ddot{\delta}_{\varphi 0}^{\text{core}} + \ddot{\delta}_{\varphi}^{\text{core}}) - (J_R^{\text{strap-on}} + m_R^{\text{strap-on}} l_R^{\text{strap-on}} \rho_C)(\ddot{\delta}_{\varphi 0}^{\text{strap-on}} + \ddot{\delta}_{\varphi}^{\text{strap-on}}) - m_z^{\alpha} q S_m l_k \alpha_w + M_z
\end{aligned}$$

Thus we have:

$$\begin{aligned}
&(\ddot{\varphi}_0 + \Delta\ddot{\varphi}) + \tfrac{J_y - J_x}{J_z}(\dot{\gamma} - \dot{\varphi}_0\psi)(\dot{\psi} + \dot{\varphi}_0\gamma) + \tfrac{m_z^{\alpha} q S_m l_k}{J_z}(\alpha_0 + \Delta\alpha) + \tfrac{m_{dz}^{\omega} q S_m l_k^2}{V J_z}(\dot{\varphi}_0 + \Delta\dot{\varphi}) \\
&+\tfrac{2P_{\text{core}}\rho_C + m_R^{\text{core}} \dot{W}_x l_R^{\text{core}}}{J_z}(\delta_{\varphi 0}^{\text{core}} + \delta_{\varphi}^{\text{core}}) + \tfrac{2P_{\text{strap-on}}\rho_C + m_R^{\text{strap-on}} \dot{W}_x l_R^{\text{strap-on}}}{J_z}(\delta_{\varphi 0}^{\text{strap-on}} + \delta_{\varphi}^{\text{strap-on}}) \\
&+\tfrac{J_R^{\text{core}} + m_R^{\text{core}} l_R^{\text{core}} \rho_C}{J_z}(\ddot{\delta}_{\varphi 0}^{\text{core}} + \ddot{\delta}_{\varphi}^{\text{core}}) + \tfrac{J_R^{\text{strap-on}} + m_R^{\text{strap-on}} l_R^{\text{strap-on}} \rho_C}{J_z}(\ddot{\delta}_{\varphi 0}^{\text{strap-on}} + \ddot{\delta}_{\varphi}^{\text{strap-on}}) \\
&+\tfrac{m_z^{\alpha} q S_m l_k}{J_z}\alpha_w = \tfrac{M_z}{J_z}
\end{aligned}$$

Considering the ideal situation:

$$\begin{aligned}
&\ddot{\varphi}_0 + \tfrac{J_y - J_x}{J_z}(\dot{\gamma} - \dot{\varphi}_0\psi)(\dot{\psi} + \dot{\varphi}_0\gamma) + \tfrac{m_z^{\alpha} q S_m l_k}{J_{z1}}\alpha_0 + \tfrac{m_{dz}^{\omega} q S_m l_k^2}{V J_{z1}}\dot{\varphi}_0 + \tfrac{2P_{\text{core}}\rho_C + m_R^{\text{core}} \dot{W}_x l_R^{\text{core}}}{J_z}\delta_{\varphi 0}^{\text{core}} \\
&+\tfrac{2P_{\text{strap-on}}\rho_C + m_R^{\text{strap-on}} \dot{W}_x l_R^{\text{strap-on}}}{J_z}\delta_{\varphi 0}^{\text{strap-on}} + \tfrac{J_R^{\text{core}} + m_R^{\text{core}} l_R^{\text{core}} \rho_C}{J_z}\ddot{\delta}_{\varphi 0}^{\text{core}} \\
&+\tfrac{J_R^{\text{strap-on}} + m_R^{\text{strap-on}} l_R^{\text{strap-on}} \rho_C}{J_z}\ddot{\delta}_{\varphi 0}^{\text{strap-on}} = 0
\end{aligned}$$

$$\begin{aligned}
&\Delta\ddot{\varphi} + \tfrac{m_{dz}^{\omega} q S_m l_k^2}{V J_z}\Delta\dot{\varphi} + \tfrac{m_z^{\alpha} q S_m l_k}{J_z}\Delta\alpha + \tfrac{2P_{\text{core}}\rho_C + m_R^{\text{core}} \dot{W}_x l_R^{\text{core}}}{J_z}\delta_{\varphi}^{\text{core}} \\
&+\tfrac{2P_{\text{strap-on}}\rho_C + m_R^{\text{strap-on}} \dot{W}_x l_R^{\text{strap-on}}}{J_z}\delta_{\varphi}^{\text{strap-on}} + \tfrac{J_R^{\text{core}} + m_R^{\text{core}} l_R^{\text{core}} \rho_C}{J_z}\ddot{\delta}_{\varphi}^{\text{core}} \\
&+\tfrac{J_R^{\text{strap-on}} + m_R^{\text{strap-on}} l_R^{\text{strap-on}} \rho_C}{J_z}\ddot{\delta}_{\varphi}^{\text{strap-on}} + \tfrac{m_z^{\alpha} q S_m l_k}{J_z}\alpha_w = \tfrac{M_z}{J_z}
\end{aligned}$$

$$\begin{aligned}
&\Delta\ddot{\varphi} + b_1^{\varphi}\Delta\dot{\varphi} + b_2^{\varphi}\Delta\alpha + b_{3\text{core}}^{\varphi}\delta_{\varphi}^{\text{core}} + b_{3\text{core}}^{\prime\varphi}\ddot{\delta}_{\varphi}^{\text{core}} + b_{3\text{strap-on}}^{\varphi}\delta_{\varphi}^{\text{strap-on}} \\
&+b_{3\text{strap-on}}^{\prime\varphi}\ddot{\delta}_{\varphi}^{\text{strap-on}} + b_2^{\varphi}\alpha_w = \overline{M}_z
\end{aligned}$$

The related coefficients are:

$$
\begin{aligned}
b_1^{\varphi} &= \frac{m_{dz}^{\omega} q S_m l_k^2}{J_z V} \\
b_2^{\varphi} &= \frac{m_z^{\alpha} q S_m l_k}{J_z} \\
b_{3\text{core}}^{\varphi} &= \frac{2P_{\text{core}}\rho_C + m_R^{\text{core}}\dot{W}_x l_R^{\text{core}}}{J_z} \\
b_{3\text{core}}^{\prime\varphi} &= \frac{J_R^{\text{core}} + m_R^{\text{core}} l_R^{\text{core}}\rho_C}{J_z} \\
b_{3\text{strap-on}}^{\prime\varphi} &= \frac{2P_{\text{strap-on}}\rho_C + m_R^{\text{strap-on}}\dot{W}_x l_R^{\text{strap-on}}}{J_z} \\
b_{3\text{strap-on}}^{\prime\varphi} &= \frac{J_R^{\text{strap-on}} + m_R^{\text{strap-on}} l_R^{\text{strap-on}}\rho_C}{J_z} \\
\overline{M}_z &= \frac{M_z}{J_z}
\end{aligned}
$$

Therefore, the formulation expression of the launch vehicle in its Pitching channel can be denoted as follows:

$$
\begin{cases}
\Delta\dot{\theta} = c_1^{\varphi}\Delta\alpha + c_2^{\varphi}\Delta\theta + c_{3\text{core}}^{\varphi}\delta_{\varphi}^{\text{core}} + c_{3\text{core}}^{\prime\varphi}\ddot{\delta}_{\varphi}^{\text{core}} + c_{3\text{strap-on}}^{\varphi}\delta_{\varphi}^{\text{strap-on}} + c_{3\text{strap-on}}^{\prime\varphi}\ddot{\delta}_{\varphi}^{\text{strap-on}} \\
+c_1^{\prime\varphi}\alpha_w + \overline{F}_{yc} \\
\Delta\ddot{\varphi} + b_1^{\varphi}\Delta\dot{\varphi} + b_2^{\varphi}\Delta\alpha + b_{3\text{core}}^{\varphi}\delta_{\varphi}^{\text{core}} + b_{3\text{core}}^{\prime\varphi}\ddot{\delta}_{\varphi}^{\text{core}} + b_{3\text{strap-on}}^{\varphi}\delta_{\varphi}^{\text{strap-on}} + b_{3\text{strap-on}}^{\prime\varphi}\ddot{\delta}_{\varphi}^{\text{strap-on}} \\
+b_2^{\varphi}\alpha_w = \overline{M}_z \\
\Delta\varphi = \Delta\alpha + \Delta\theta
\end{cases}
$$

Similarly, we have the linearized model in other channels.
In the Yawing channel:

$$
\begin{cases}
\dot{\sigma} = c_1^{\psi}\beta + c_2^{\psi}\sigma + c_{3\text{core}}^{\psi}\delta_{\psi}^{\text{core}} + c_{3\text{core}}^{\prime\psi}\ddot{\delta}_{\psi}^{\text{core}} + c_{3\text{strap-on}}^{\psi}\delta_{\psi}^{\text{strap-on}} + c_{3\text{strap-on}}^{\prime\psi}\ddot{\delta}_{\psi}^{\text{strap-on}} \\
+c_1^{\prime\psi}\beta_w - \bar{F}_{zc} \\
\ddot{\psi} + b_1^{\psi}\dot{\psi} + b_2^{\psi}\beta + b_{3\text{core}}^{\psi}\delta_{\psi}^{\text{core}} + b_{3\text{core}}^{\prime\psi}\ddot{\delta}_{\psi}^{\text{core}} + b_{3\text{strap-on}}^{\psi}\delta_{\psi}^{\text{strap-on}} + b_{3\text{strap-on}}^{\prime\psi}\ddot{\delta}_{\psi}^{\text{strap-on}} \\
+b_2^{\psi}\beta_w = \bar{M}_y \\
\psi = \beta + \sigma
\end{cases}
$$

and in Rolling channel:

$$
\ddot{\gamma} + d_1\dot{\gamma} + d_{3\text{core}}\delta_{\gamma}^{\text{core}} + d_{3\text{core}}^{\prime}\ddot{\delta}_{\gamma}^{\text{core}} + d_{3\text{strap-on}}\delta_{\gamma}^{\text{strap-on}} + d_{3\text{strap-on}}^{\prime}\ddot{\delta}_{\gamma}^{\text{strap-on}} = \bar{M}_x.
$$

## References


1. Cheng T, Wang X, Li D (2003) The new generation launch vehicles of long march family. In: The 54th international astronautical congress of the International Astronautical Federation, Bremen, Germany
2. Patton RJ (1993) Robustness issues in fault tolerant control. In: The processing of international conference on fault diagnosis, Toulouse, France, pp 1081–1117
3. Stengel RR (1991) Intelligent failure tolerant control. IEEE Control Syst Mag 11(3):14–23
4. Vidyasagar M (1987) Some results on simultaneous stabilization with multiple domains of stability. Automatica 23:535–540
5. Wang Z, Zhao DJ, Wang YJ, Liu DB (2012) Reconfiguration of shipboard power system using discrete particle swarm optimisation. Int J Model Identif Control 15(4):277–283
6. Wu DN, Gao WB, Chen M (1990) Algorithm for simultaneous stabilization of single-input systems via dynamic feedback. Int J Control 51(3):631–642
7. Vishwakarma R, Turner D, Lewis A, Chen YK, Xu YG (2012) The use of pseudo-inverse methods in reconstructing loads on a missile structure. Int J Model Identif Control 17(3): 242–250
8. Wang ZJ, Guo SJ (2012) Rolling flight control using pseudo inverse control allocation for UAVs with multiple seamless warping control surfaces. Int J Model Identif Control 16(1):15–23
9. Pei Y, Li PQ, Yao YP (1998) The application of function reconfiguration for digital fly-by-wire flight control system. In: The proceedings of the 17th Digital Avionics Systems conference, pp 76–81
10. Gopinathan M, Boskovic JD, Mehra RK, Rago C (1998) A multiple model predictive scheme for fault-tolerant flight control design. In: The proceedings of the 37th IEEE conference on decision and control, pp 1376–1381
11. Chandler P, Mears M, Pachter M (1994) On-line optimizing networks for reconfiguratable control. AIAA-94-3643-CP, pp 263–268
12. Chen Z, Hao LN, Xue DY, Xu XH, Liu YM (2011) Real-time compensation control for hysteresis and creep in IPMC actuators. Int J Model Identif Control 12(1/2):182–189
13. Jiang Y, Hu Q, Ma G (2008) Design of robust adaptive integral variable structure attitude controller with application to flexible spacecraft. Int J Innov Comput Inf Control 4(9): 2431–2440
14. Kemih K, Merabtine N, Benslama M, Filali S (2007) Generalized predictive control using conjugate gradient method applied to micro satellites attitude control. ICIC Express Lett 1(2): 99–104
15. Marcello R, Nitin D, Gao Z (1994) On-line learning non-linear direct neural controllers for reconstrucible control systems. AIAA-94-3643-CP, pp 141–147
16. Gao Z, Jiang B, Shi P, Xu Y (2010) Fault accommodation for near space vehicle attitude dynamics via T-S fuzzy models. Int J Innov Comput Inf Control 6(11):4843–4856
17. Sadeghi T, Lai K (1995) Integrated fault tolerant control law. In: The proceedings of the IEEE 1995 national aerospace and electronics conference, pp 491–512
18. Robert C, Eslinger A, Chandler PR (1993) Self-repairing flight control system overview. IEEE Trans Autom Control 4:143–151
19. Du F, Wang X, Sun H (2008) Fault-tolerant control on missile rudder deadlock. J Proj Rockets Missiles Guidance 28(5):67–70
20. Das RK, Sen S, Dasgupta S (2007) Robust and fault tolerant controller for attitude control of a satellite launch vehicle. IET Control Theory Appl 1(1):304–312
21. Blakelock JH (1991) Automatic control aircraft and missile. A Wiley-Interscience, New York
22. Nelson RC (1989) Flight stability and automatic control. McGraw-Hill Book Company, New York
23. Wu Y, He L (2009) Attitude control technology of new generation launch vehicles. J Beijing Univ Aeronaut Astronaut 35(11):1294–1297
24. Xu Y (1999) Ballistic Missile, Launch vehicle control system design and analysis. China Astronautic Publishing House, Beijing

http://www.springer.com/978-3-642-36384-9

Applied Methods and Techniques for Mechatronic Systems
Modelling, Identification and Control
Liu, L.; Zhu, Q.; Cheng, L.; Wang, Y.; Zhao, D. (Eds.)
2014, XV, 440 p. 251 illus., Softcover
ISBN: 978-3-642-36384-9